SCHEDULING CAPACITY ENHANCEMENT FOR NEXT GENERATION NARROWBAND IOT THROUGH SUBCARRIER SPACING REDUCTION

by

Md. Rafat Bin Rabbani (160021007)
Md. Asif Ishrak Sarder (160021013)
Hossain Md. Mubashshir Jamil (160021046)

A Thesis Submitted to the Academic Faculty in Partial Fulfillment of the Requirements for the Degree of

BACHELOR OF SCIENCE IN ELECTRICAL AND ELECTRONIC ENGINEERING

Department of Electrical and Electronic Engineering
Islamic University of Technology (IUT)
Gazipur, Bangladesh

March 2021

SCHEDULING CAPACITY ENHANCEMENT FOR NEXT GENERATION NARROWBAND IOT THROUGH SUBCARRIER SPACING REDUCTION

Approved by:

Tawhid

Dr. Mohammad Tawhid Kawser

Supervisor and Professor
Department of Electrical and Electronic Engineering
Islamic University of Technology (IUT)
Boardbazar, Gazipur-1704.

Date: ……

Table of Contents

List of Tables ..... **iv**

List of Figure ..... **v**

List of Acronyms ..... **vii**

Acknowledgements ..... **x**

Abstract ..... **xi**

1 Introduction **1**

1.1 Growing Importance of Massive IoT 1
1.2 Enabling Technologies for Massive IoT 4
1.3 A Primer on Narrowband IoT 5
1.4 Research Motivation 7
1.5 Related Work 8
1.6 Research Objectives 9

2 NB-IoT: System Overview **10**

2.1 Deployment Scheme 10
2.1.1 Modes of Operation *10*

2.1.1.1 In-band Mode **10**

2.1.1.2 Guard-band Mode **11**

2.1.1.3 Stand-alone Mode **11**

2.1.2 Carrier Raster: *12*
2.1.3 FDD Deployment: *12*
2.1.4 Repetitions: *12*
2.2 Resource Grid Structure: 12
2.2.1 DL Resource Grid: *12*
2.2.2 UL Resource Grid: *14*
2.3 DL Physical Channels and Signals: 16
2.3.1 NPSS & NSSS: *16*
2.3.2 NRS: *17*
2.3.3 NPRS: *17*
2.3.4 NPBCH: *17*
2.3.5 NPDCCH: *17*
2.3.6 NPDSCH: *18*
2.4 UL Physical Channels and Signals: 18
2.4.1 NPRACH: *18*
2.4.2 NPUSCH: *19*
2.4.3 DMRS: *19*

3 Methodology **21**

3.1 Design Considerations 21
3.1.1 DMRS Positioning: *21*
3.1.2 Length of CP: *22*

3.1.3 Presence of GP: *22*
3.2 PROPOSED SCHEME: 23
4 Software based Performance Testing 25
4.1 STANDALONE DEPLOYMENT: 26
4.1.1 Standalone BER vs SNR: *27*
4.1.2 Standalone FER vs SNR: *29*
4.1.3 Standalone Throughput vs SNR: *31*
4.1.4 Standalone CEE vs SNR: *33*
4.1.5 Standalone P vs PAPR: *35*
4.2 IN-BAND DEPLOYMENT 37
4.2.1 In-band BER vs SNR: *39*
4.2.2 In-band FER vs SNR: *41*
4.2.3 In-band Throughput vs SNR: *43*
4.2.4 In-band CEE vs SNR: *45*
4.2.5 In-band P vs PAPR: *47*
4.3 GUARD-BAND DEPLOYMENT 49
4.3.1 Guard-band BER vs SNR: *50*
4.3.2 Guard-band FER vs SNR: *52*
4.3.3 Guard-band Throughput vs SNR: *54*
4.3.4 Guard-band CEE vs SNR: *56*
4.3.5 Guard-band P vs PAPR: *58*
5 Chapter 5 60
6 Conclusion 60
7 References 61

List of Tables

Table 4.1: Permitted GSM bands and their LTE equivalents for NB-IoT standalone deployment....26
Table 4.2: Standalone BER comparison....28
Table 4.3: Standalone FER comparison....30
Table 4.4: Standalone throughput comparison....32
Table 4.6: Standalone PAPR comparison....36
Table 4.8: In-band BER comparison....40
Table 4.9: In-band FER comparison....42
Table 4.10: In-band throughput comparison....44
Table 4.11: In-band CEE comparison....46
Table 4.12: In-band PAPR comparison....48
Table 4.13: Guard-band BER comparison....51
Table 4.14: Guard-band FER comparison....53
Table 4.15: Guard-band throughput comparison....55
Table 4.16: Guard-band CEE comparison....57
Table 4.17: Guard-band PAPR comparison....59

List of Figures

Figure 1.1: Massive IoT Connectivity Use Cases 1
Figure 1.2: Massive IoT Growth Predictions 2
Figure 1.3: 5G Usage Scenarios & Key Capabilities of IMT-2020 4
Figure 2.1: Channel and Transmission Bandwidth for In-band Mode operation. 10
Figure 2.2: Channel and Transmission Bandwidth for Guard-band Mode operation. 11
Figure 2.3: Channel and Transmission Bandwidth for Stand-alone Mode operation. 11
Figure 2.4: Downlink Resource Grid (with 15 kHz subcarrier spacing).....13
Figure 2.5: Uplink Resource Grid (with 15 kHz subcarrier spacing).....14
Figure 2.6: Uplink Resource Grid (with 3.75 kHz subcarrier spacing).....15
Figure 2.7: Downlink Resource Scheduling (with 15 kHz subcarrier spacing) 18
Figure 2.8: Uplink Resource Scheduling (In-band Mode) 20
Figure 3.1: Data/DMRS symbol arrangement in scaled slot/subframe for 1.875 kHz subcarrier spacing 22
Figure 3.2: Cyclic Prefix/ Guard Period Dimension 22
Figure 3.3: Proposed Uplink resource Grid (with 1.875 kHz Subcarrier Spacing).....23
Fig 4.1: Already existing 15kHz SCS uplink BER in standalone mode 27
Fig 4.2: Already existing 3.75kHz SCS uplink BER in standalone mode 27
Fig 4.3: Our Proposed 1.875kHz SCS uplink BER in standalone mode.....28
Fig 4.4: Already existing 15kHz SCS uplink FER in standalone mode.....29
Fig 4.5: Already existing 3.75kHz SCS uplink FER in standalone mode.....29
Fig 4.6: Our Proposed 1.875kHz SCS uplink FER in standalone mode 30
Fig 4.7: Already existing 15kHz SCS uplink throughput in standalone mode.....31
Fig 4.8: Already existing 3.75kHz SCS uplink throughput in standalone mode.....31
Fig 4.9: Our Proposed 1.875kHz SCS uplink throughput in standalone mode 32
Fig 4.10: Already existing 15kHz SCS uplink CEE in standalone mode.....33
Fig 4.11: Already existing 3.75kHz SCS uplink CEE in standalone mode.....33
Fig 4.12: Our Proposed 1.875kHz SCS uplink CEE in standalone mode 34
Fig 4.13: Already existing 15kHz SCS uplink PAPR in standalone mode 35
Fig 4.14: Already existing 3.75kHz SCS uplink PAPR in standalone mode 35
Fig 4.15: Our Proposed 1.875kHz SCS uplink PAPR in standalone mode.....36
Fig 4.16: Already existing 15kHz SCS uplink BER in in-band mode 39
Fig 4.17: Already existing 3.75kHz SCS uplink BER in in-band mode 39
Fig 4.18: Our Proposed 1.875kHz SCS uplink BER in in-band mode.....40
Fig 4.19: Already existing 15kHz SCS uplink FER in in-band mode.....41
Fig 4.20: Already existing 3.75kHz SCS uplink FER in in-band mode.....41
Fig 4.21: Our Proposed 1.875kHz SCS uplink BER in in-band mode.....42
Fig 4.22: Already existing 15kHz SCS uplink throughput in in-band mode.....43
Fig 4.23: Already existing 3.75kHz SCS uplink throughput in in-band mode.....43
Fig 4.24: Our Proposed 1.875kHz SCS uplink throughput in in-band mode 44
Fig 4.25: Already existing 15kHz SCS uplink CEE in in-band mode.....45
Fig 4.26: Already existing 3.75kHz SCS uplink CEE in in-band mode.....45
Fig 4.27: Our Proposed 1.875kHz SCS uplink CEE in in-band mode 46
Fig 4.28: Already existing 15kHz SCS uplink PAPR in in-band mode 47
Fig 4.29: Already existing 3.75kHz SCS uplink PAPR in in-band mode 47
Fig 4.30: Our Proposed 1.875kHz SCS uplink PAPR in in-band mode.....48
Fig 4.31: Already existing 15kHz SCS uplink BER in Guard-band mode 50
Fig 4.32: Already existing 3.75kHz SCS uplink BER in Guard-band mode 50

Fig 4.33: Our Proposed 1.875kHz SCS uplink BER in Guard-band mode.....51
Fig 4.34: Already existing 15kHz SCS uplink FER in Guard-band mode.....52
Fig 4.35: Already existing 3.75kHz SCS uplink FER in Guard-band mode.....52
Fig 4.36: Our Proposed 1.875kHz SCS uplink FER in Guard-band mode 53
Fig 4.37: Already existing 15kHz SCS uplink throughput in Guard-band mode.....54
Fig 4.38: Already existing 3.75kHz SCS uplink throughput in Guard-band mode.....54
Fig 4.39: Our Proposed 1.875kHz SCS uplink throughput in Guard-band mode 55
Fig 4.40: Already existing 15kHz SCS uplink CEE in Guard-band mode.....56
Fig 4.41: Already existing 3.75kHz SCS uplink CEE in Guard-band mode.....56
Fig 4.42: Our Proposed 1.875kHz SCS uplink CEE in Guard-band mode 57
Fig 4.43: Already existing 15kHz SCS uplink PAPR in Guard-band mode 58
Fig 4.44: Already existing 3.75kHz SCS uplink PAPR in Guard-band mode 58
Fig 4.45: Our Proposed 1.875kHz SCS uplink PAPR in Guard-band mode.....59

List of Acronyms

3GPP	3rd Generation Partnership Project
ACK	Acknowledgement
BCH	Broadcast Channel
BER	Bit Error Rate
BPSK	Binary Phase Shift Keying
BU	Bottom-Up power filling
CDF	Cumulative Distribution Function
CEE	Channel Estimation Error
CP	Cyclic Prefix
CRS	Cell-Specific Reference Signal
CSS	Chirp Spread Spectrum
DBPSK	Differential Binary Phase-Shift Keying
DL	Downlink
DMRS	Demodulation Reference Signal
EC	Extended Coverage
eDRX	Extended Discontinuous Reception
eMTC	Enhanced Machine Type Communication
Fast-OFDM	Fast-Orthogonal Frequency Division Multiplexing
FDD	Frequency-Division Duplexing
FER	Frame Error Rate
GFSK	Gaussian Frequency Shift Keying
GP	Guard Period
GPRS	General Packet Radio Service
GSM	Global System for Mobile *Communication*
IC	Item Clustering
ICI	Inter-channel interference
IMT	International Mobile Telecommunication
ISI	Inter-Symbol-Interference
ISM	Industrial, Scientific and Medical
ITU	International Telecommunication Union

ITU-R	ITU Radiocommunication Sector
LPWAN	Low-Power Wide-Area Network
LTE	Long Term Evolution
MCL	Maximum Coupling Loss
MIB	Master Information Block
mIoT	Massive Internet-of-Things
mMTC	massive Machine-Type Communications
NACK	Negative Acknowledgement
NB-IoT	Narrowband Internet-of-Things
NOMA	Non-orthogonal Multiple Access
NPBCH	Narrowband Physical Broadcast Channel
NPDCCH	Narrowband Physical Downlink Control Channel
NPDSCH	Narrowband Physical Downlink Shared Channel
NPRACH	Narrowband Physical Random Access Channel
NPRS	Narrowband Positioning Reference Signal
NPSS	Narrowband Primary Synchronization Signal
NPUSCH	Narrowband Physical Uplink Shared Channel
NRS	Narrowband Reference Signal
NSSS	Narrowband Secondary Synchronization Signal
OFDM	Orthogonal Frequency Division Multiplexing
OFDMA	Orthogonal Frequency Division Multiple Access
PA	Power Amplifier
PAPR	Peak-To-Average Power Ratio
PDCCH	Physical Downlink Control Channel
PRB	Physical Resource Block
PSD	Power Spectral Density
PSK	Phase Shift Keying
PSM	Power Saving Mode
QPSK	Quadrature Phase Shift Keying
RAR	Random Access Response
RU	Resource Unit
SC-FDMA	Single Carrier Frequency Division Multiple Access

SCS	Subcarrier Spacing
SEFDM	Spectrally Efficient Frequency Division Multiplexing
SIB	System Information Block
SINR	Signal To Noise Ratio
SNR	Signal To Noise Ratio
SRD	Short Range Device
SRS	Sounding Reference Signal
TDD	Time-Division Duplexing
UE	User Equipment
UL	Uplink
UNB	Ultra Narrow Band
WSIG	Weightless Special Interest Group

Acknowledgements

We would like to thank our supervisor Dr. Mohammad Tawhid Kawser, Professor, Department of EEE, IUT for providing precious guidance, inspiring discussions and constant supervision throughout the course of this work. His help, constructive criticism, and conscientious efforts made it possible for us to present the work. It's our goodness that in spite of having a tight and busy schedule our supervisor has found time to help and guide us. For this, we again express our sincere gratitude to him. We are also grateful to EEE Department of IUT for providing us the opportunity to present this work.

Abstract

Meeting the requirements of the Low-Power Wide Area Network (LPWAN), Narrowband Internet of Things (NB-IoT) is the most promising technology being come across to date. Currently, the NB-IoT framework is operating on 180 kHz bandwidth with 15 kHz subcarrier spacing using OFDM for Downlink and 3.75 kHz and 15 kHz subcarrier spacing using SC-FDMA for Uplink respectively for single-tone and multi-tone transmission. Several research activities have already pointed to several lacking of the current NB-IoT framework. In this manuscript, firstly, the design of the current framework of NB-IoT is discussed. Secondly, to ensure an increment in the number of connected UEs, we proposed a modified resource grid over the current scheme using the 1.875 kHz subcarrier spacing for the single-tone uplink data transmission and investigated its performance under different scenarios using Vienna 5G Link Level Simulator.

Chapter 1

Introduction

In this chapter, the reader is introduced to some background, motivation and key research goals for the work presented in this thesis.

1.1 Growing Importance of Massive IoT

The term “Massive Internet-of-Things”, often used interchangeably with “massive Machine-Type Communications” (mMTC) in the 5G world, is a category driven by scale rather than speed. It is characterized by a very large number of connections, small data volumes, low-cost devices and limited energy consumption requirements. Massive IoT applications are typically less latency sensitive and have relatively low throughput requirements. Figure 1.1[1] depicts the wide range of mIoT application areas presented in the upcoming sections.

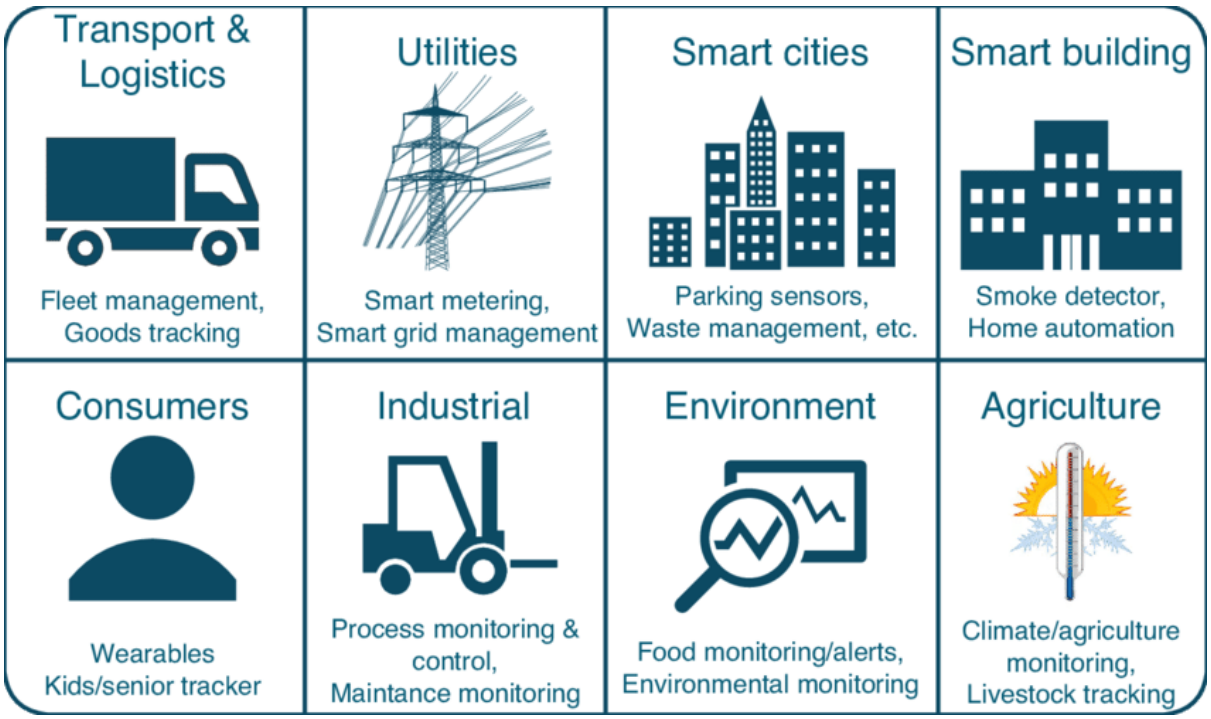

Figure 1.1: Massive IoT Connectivity Use Cases

1. **Transport & Logistics:** An important mIoT use case is in the global supply chains. In the coming days, IoT sensors will automate the movement of goods and optimize the delivery routes for many e-commerce players in the market. In some cases, low-power IoT sensors are already being used to track assets in real time throughout the supply chain and monitor product quality by measuring temperature, vibration, leakage, etc.

2. **Utilities:** Smart utilities with connected sensors are one of the earliest IoT adopters. Nowadays we are seeing utility service providers using smart meters to optimize energy distribution and improve the overall efficiency. The customers are also being benefitted by the actionable insights they are receiving on their energy usage.

3. **Smart Cities:** One of the most promising mIoT use cases would be in creating smarter, more efficient cities. Cities monitored and managed by a network of smart sensors can improve public services and enhance the quality of life for the citizens. Public transportation, waste management, water supply monitoring, etc. are some of the key application areas that can utilize the full potential of a smart connected sensor network.

4. **Smart Buildings:** Building automation improves the operational and cost efficiencies by providing the facility owners with the ability to manage building operations through IoT networks. A system of smart sensors can help the operators and managers reduce maintenance costs with predictive maintenance, enhance security, and make the buildings more energy efficient and sustainable.

5. **Consumers:** A range of always-on and always-connected personal devices are being used by people around the world to track, manage and secure sensitive health and other personal data. Right now, this market is being driven by the mass adoption of smart wearables such as smart watches, fitness trackers, etc. But very soon, we expect to see new innovations and application areas in this segment.

6. **Industrial:** Manufacturing industry is one of the areas that can highly benefit from the adoption of mIoT. Smart factories will help owners reduce the overall carbon footprint through efficient inventory planning and optimization. Automated machine

maintenance and operations, faster identification of performance issues and improved worker safety will drive sustainable business growth in the near future.

7. **Environment:** Scalable and robust networks of connected sensors are enabling modern-day environmental monitoring applications. These networks are being used to monitor and prevent deforestation and preserve biodiversity and ecosystems, which, in turn, are helping us combat climate change and create a more sustainable environment.

8. **Agriculture:** IoT has revolutionized the global agriculture sector by helping farmers improve operational efficiencies and maximize crop yields. Remote crop monitoring and livestock tracking improve overall productivity. Smart farming has empowered small farmers with tools for food safety and security.

The deployment of massive IoT networks is well underway across the globe and many of the application areas described above are already being powered by these networks. Figure 1.2 [2] shows the growth predictions for mIoT devices from 2021 until 2026. Ericsson predicts that by the end of 2021, there will be around 374 million mIoT connections worldwide and that number is projected to reach 2.67 billion in 2026.

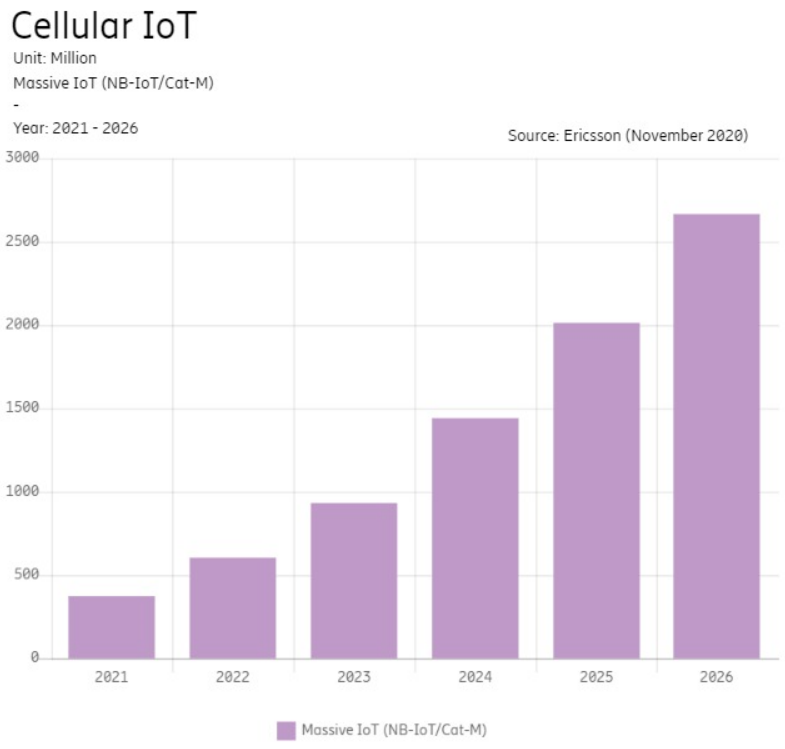

Figure 1.2: Massive IoT Growth Predictions

Market analysts predict that in the coming years, growth in the number of connected mIoT devices will eclipse that of all other forms of IoT applications. Because various open standard and proprietary Low-Power Wide-Area Network (LPWAN) technologies are already available to support the needs of massive IoT applications. Hence, we are going to see a whole range of new innovations and mass adoption in this particular area in the near future.

So, the importance of massive IoT will rise exponentially in the next few years, and thus any research input in this field is going to be particularly valuable.

1.2 Enabling Technologies for Massive IoT

Massive IoT applications are a natural fit for Low-Power Wide-Area Networks (LPWANs). These network technologies match the key requirements of a massive IoT deployment and many of them can provide ubiquitous coverage by utilizing existing cellular infrastructures. There are several technologies that enable LPWA networks in both unlicensed and licensed spectrum; some of the most promising ones are summarized in the sections below.

1. **Sigfox:** SIGFOX created the Ultra Narrow Band (UNB) radio modulation technology as a wide area wireless access technology, to support a massive number of low-power IoT devices. For transmission, Sigfox uses ultra-narrowband channels of 100 Hz in the publicly available ISM band and provides data rates from 100 bps to 600 bps. It employs Differential Binary Phase-Shift Keying (DBPSK) and Gaussian Frequency Shift Keying (GFSK), and supports coupling loss higher than 160 dB. Sigfox networks follow a client-server model with one-hop star topology that maximizes battery life [3].

2. **LoRa & LoRaWAN:** LoRa is a physical layer modulation technique and LoRaWAN is a set of protocols designed for the MAC layer and the network layer; both of them are supported and maintained by the LoRa Alliance. LoRa uses chirp spread spectrum (CSS) based modulation technique for data transmission on channels of 125 kHz bandwidth in the license-free SRD bands. It supports a maximum coupling loss of 157 dB [4] and provides data rates of up to 50 kbps [1].

3. **Weightless:** Weightless is an open standard narrowband LPWAN technology developed by Weightless Special Interest Group (WSIG). It employs a lightweight

protocol stack to minimize the transmission overhead which makes it particularly well suited for massive IoT applications. The latest set of standards supports both network-originated and device-originated transmission on 12.5 kHz narrowband channels in the unlicensed sub-GHz ISM/SRD bands. It uses PSK/GMSK modulation with spread spectrum and frequency hopping techniques to provide adaptive data rates from 625 bps to 100 kbps [40].

4. **EC-GSM-IoT:** Extended Coverage GSM IoT (EC-GSM-IoT) is an LPWA technology based on eGPRS. It has been standardized in 3GPP release 13 for use in licensed spectrum. Originally designed as a high capacity, long range and low complexity cellular system to support massive IoT, EC-GSM-IoT operates on 200 kHz channel bandwidth in GSM bands and can facilitate data rates up to 70 kbps with GMSK modulation and 240 kbps with 8-PSK modulation schemes in both uplink and downlink. It supports a range of latency from 700 milliseconds to 2 seconds [41].

5. **LTE-M (eMTC):** LTE-M, formally known as eMTC (enhanced Machine Type Communication), is a set of standards that enables massive IoT networks utilizing existing LTE infrastructures. It was also standardized in 3GPP release 13. Operating on 1.4 MHz bandwidth, LTE-M supports a Maximum Coupling Loss (MCL) of 155 dB and offers data rates of up to 300 kbps in the downlink and 375 kbps in the uplink [5].

1.3 A Primer on Narrowband IoT

Narrowband Internet-of-Things (NB-IoT), developed and maintained by the 3rd Generation Partnership Project (3GPP), is an LPWAN radio technology standard that focuses on massive IoT applications with low data throughput requirements.

A high-level summary of the main NB-IoT features is presented below, with a focus on how these features attempt to achieve the various massive IoT design goals.

1. **Narrowband Operation:** For NB-IoT, the operating bandwidth is restricted to 180 kHz which can facilitate low data rate applications. NB-IoT employs Orthogonal Frequency Division Multiplexing (OFDM) principle where the total channel bandwidth is split into a number of orthogonal subcarriers. Each of these subcarriers can carry data to different recipients without interfering with each other. Thus, this technique

introduces unparalleled spectral efficiency, minimizes the transceiver complexity and cost, and facilitates high user density.

2. **Half Duplex Operation:** Half-duplex operation reduces the device complexity and brings down the production cost of NB-IoT UEs significantly.

3. **Discontinuous Reception and Transmission:** Power Saving Mode (PSM) and Extended Discontinuous Reception (eDRX) minimize power consumption of NB-IoT UEs, which, in turn, facilitates longer battery life.

4. **Repetition in Signal Transmissions:** In NB-IoT, data is transmitted several times to increase the probability of successful decoding of the transmitted message. This feature boosts coverage in areas of poor signal reception.

5. **Variable Subcarrier Spacing:** NB-IoT uses Single Carrier Frequency Division Multiple Access (SC-FDMA) in the uplink and Orthogonal Frequency Division Multiple Access (OFDMA) technique in the downlink for data transmission. It employs Power Spectral Density (PSD) boosting in the uplink with a subcarrier spacing configuration of 3.75 kHz. The downlink only supports the legacy 15 kHz subcarrier spacing.

6. **Flexible Resource Scheduling:** The majority of the massive IoT applications will be uplink-oriented. To support a high number of devices with variable throughput and latency requirements within a single Physical Resource Block (PRB) in the uplink, the network leverages the flexibility NB-IoT offers in radio resource scheduling. The eNodeB can schedule 1, 3, 6 or 12 contiguous subcarriers, i.e., multi-tone scheduling, with 15 kHz spacing to individual NB-IoT UEs. Furthermore, with 3.75 kHz subcarrier spacing, 48 subcarriers can be separately allocated which is known as single-tone scheduling. This flexibility increases the system's capacity to handle a large number of connections at any given time.

1.4 Research Motivation

The three usage scenarios specified by the ITU Radiocommunication Sector (ITU-R) for the 5G wireless standards (termed as IMT-2020) are depicted in Figure 1.3 [6]. These scenarios are Enhanced Mobile Broadband, Massive Machine-Type Communications (massive IoT), and Ultra-Reliable and Low-Latency Communications (critical IoT). NB-IoT, although first designed as a part of the LTE specifications in release 13, is now being used as the foundation for further enhancements to meet the key requirements of the massive IoT use cases in the 5G wireless standards.

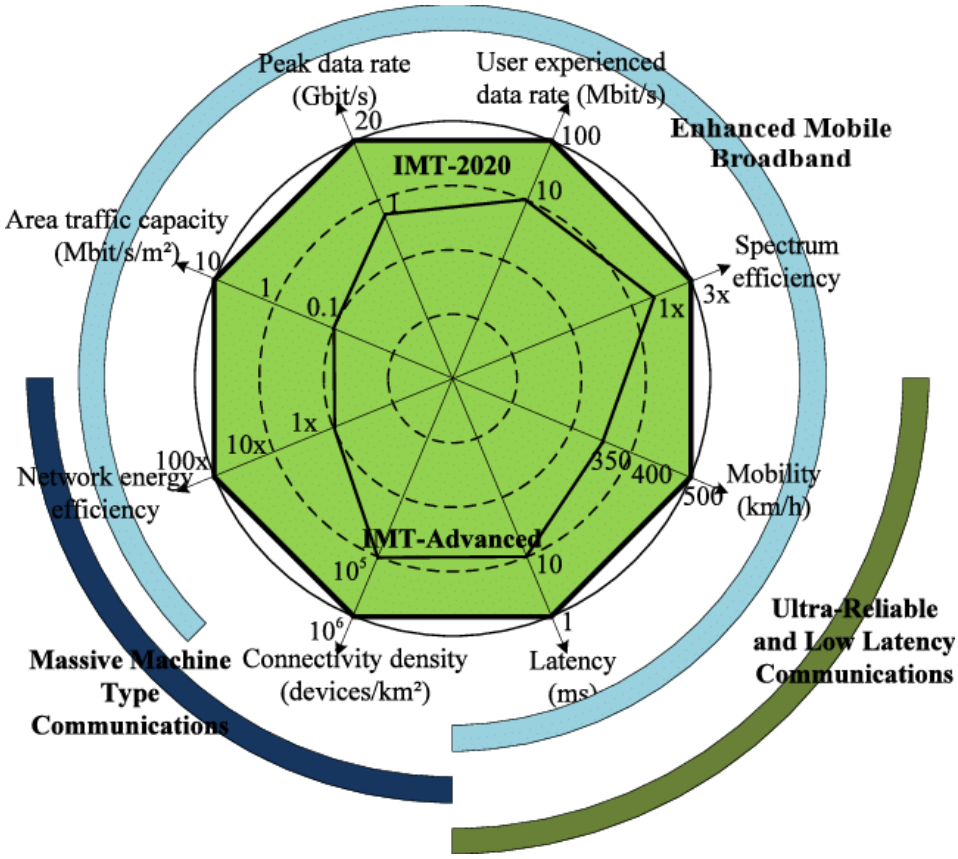

Figure 1.3: 5G Usage Scenarios & Key Capabilities of IMT-2020

One of the key requirements of IMT-2020 standard is the support for 1 million connected devices per square kilometer with a maximum latency of 10 seconds. But current deployments of NB-IoT on existing LTE infrastructures can only handle up to 50,000 connected devices per cell [7]. To meet the huge IoT connection density requirement, in this

work, a new physical layer resource grid based on a subcarrier spacing of 1.875 kHz is proposed which can essentially double the number of NB-IoT devices the eNodeB can serve at a time.

1.5 Related Work

Some rudimental studies have already investigated the device capacity of NB-IoT, and for maximizing the connection density, a variety of schemes have been come-up. One of them is Non-orthogonal Multiple Access (NOMA) [8]. A heuristic solution has been proposed in [9] using the power-domain NOMA scheme where two IoT devices are allowed to access one subcarrier simultaneously. Nevertheless, issues like Inter-channel interference (ICI) reduce supported connection density due to the fact that higher data rate requirements remain extant. Another work in [10] introduces Bottom-Up power filling (BU) and a novel Item Clustering (IC) based approach for maximizing connection density. However, better performance from this approach comes up with a little compromisation as an increment in peak-to-average power ratio (PAPR) in the uplink.

Works of [11],[12] indicates the availability of another scheme called fast-orthogonal frequency division multiplexing (Fast-OFDM) [13]. A study in [11] claims the achievement of potentially doubling the number of connected IoT devices by compressing the occupied bandwidth, precisely half of that in OFDM. Reference [12] also adopts Fast-OFDM waveform for a new framework named enhanced NB-IoT (eNB-IoT), where occupied bandwidth is halved for a particular data rate, reaching the same BER, without using the repetitive transmission procedure. However, the only feasible modulation scheme for Fast-OFDM is BPSK, which is a bit deficient to $\pi/2$-BPSK available for SC-FDMA in uplink in case of peak-to-average power ratio (PAPR) [14].

Another promising scheme is the Spectrally Efficient Frequency Division Multiplexing (SEFDM) [15], which offers non-orthogonal signal waveform, improving data rate without upgrading modulation formats greater than QPSK [16] by gaining spectral efficiency over OFDM [17]. But the deliberate violation of the orthogonality of the subcarriers causes issues such as amelioration of the effects of Inter-carrier Interference (ICI), degradation in channel estimation, which can be mitigated at a certain level at the expense of involvement of compound approach [18], receiver complexity [19], increased pilot duration overhead [20].

1.6 Research Objectives

The research objectives of this thesis can be stated as follows:

1. Design and optimization of a new physical layer channel structure and resource grid based on 1.875 kHz subcarrier spacing for NB-IoT to enhance its resource scheduling capacity.
2. Assessment of the feasibility of the newly designed resource grid and its coexistence with the existing physical layer infrastructures.

Chapter 2

NB-IoT: System Overview

2.1 Deployment Scheme

In this section, operating systems of NB-IoT technology for both downlink and uplink transmission have been discussed.

2.1.1 Modes of Operation

Taking into account the consideration of optimization in parallel, the basic frame structure and substantial numerologies and deployment schemes of NB-IoT have been developed from the framework of legacy LTE.

According to the specifications provided by the 3GPP in its Release 13 [21], the deployment schemes of NB-IoT depend upon three disparate operating bands. They are discussed in the following sections.

2.1.1.1 In-band Mode

For both downlink and uplink transmission, only one PRB is allocated within the existing LTE carrier in this operating mode. However, NB-IoT cannot use the PRBs allocated for LTE CRS and LTE PDCCH [22]. The channel bandwidth ranges from 3 MHz to 20 MHz, and the transmission bandwidth is 180 kHz [23].

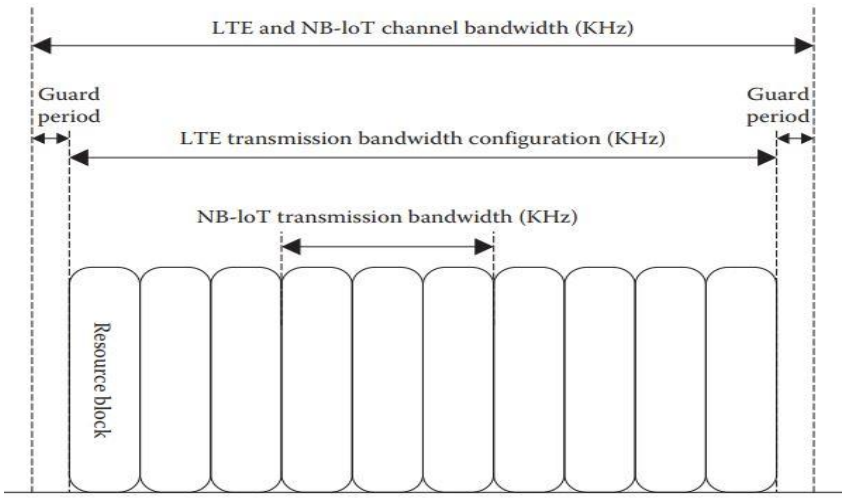

Figure 2.1: Channel and Transmission Bandwidth for In-band Mode operation.

2.1.1.2 Guard-band Mode

For the NB-IoT data transmission, either of the two unused guard bands situated at two ends of the whole legacy LTE carrier can be allocated in this operating mode. Similar to In-band mode, only one PRB of 180 kHz of LTE can be used for NB-IoT in this mode. In the frequency domain, the operating range is from 4 MHz to 20 MHz[23].

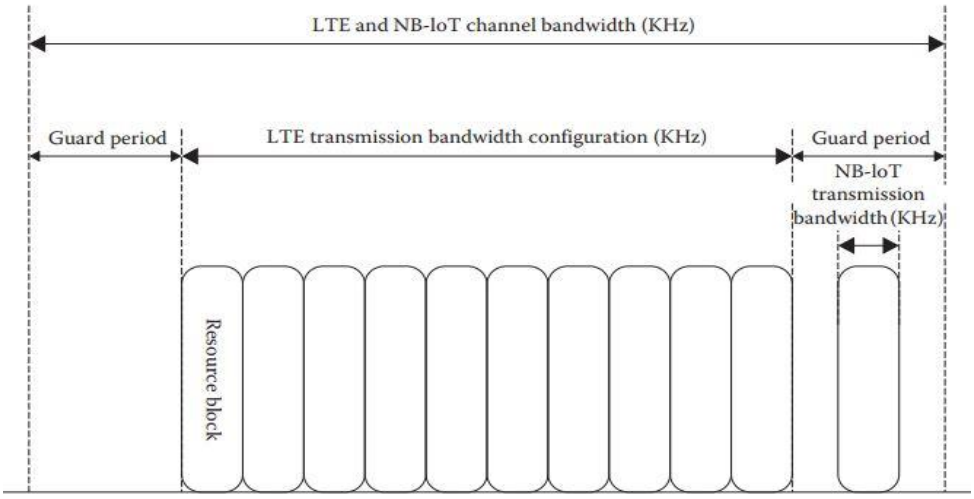

Figure 2.2: Channel and Transmission Bandwidth for Guard-band Mode operation.

2.1.1.3 Stand-alone Mode

In the case of data transmission, NB-IoT can make use of a 200 kHz channel bandwidth by replacing unused GSM carriers in this operating mode. The transmission bandwidth is 180 kHz. Similar to the earlier guard-band mode, this operation has no impact on the existing LTE bandwidth.

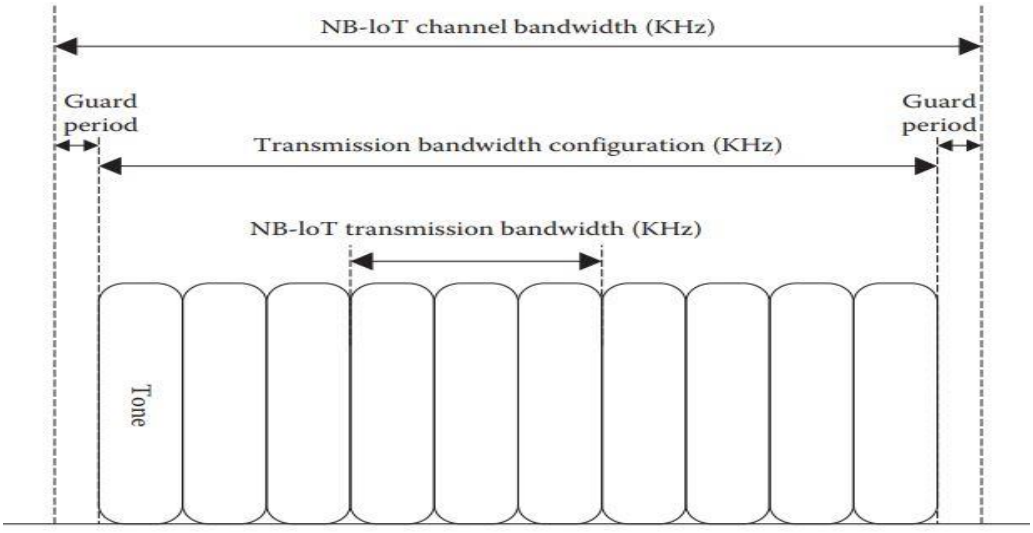

Figure 2.3: Channel and Transmission Bandwidth for Stand-alone Mode operation.

2.1.2 Carrier Raster:

Carrier raster is utilized for interpreting necessary frequency difference between center frequencies of different carriers. Like LTE UEs, NB-IoT UE is only authorized to employ a 100 kHz raster to pursue for a carrier for all three abovementioned operating schemes[21].

2.1.3 FDD Deployment:

According to the 3GPP release 13, as for the duplex mode, Frequency-Division Duplexing (FDD) mode was chosen for the NB-IoT system[24]. Following the Release 15, Time-Division Duplexing (TDD) feature has already been introduced to the NB-IoT system[25].

2.1.4 Repetitions:

In order to achieve further coverage extension and increment in the probability of successful data reception, the scheme of repetition of the same signal is adopted. A maximum of 2048 and 128 repetitions are allowed for the Downlink and Uplink transmission, discretely[26].

2.2 Resource Grid Structure:

While operating and allocating resources based upon a framework, to establish coexistence with the LTE, NB-IoT has adapted the signals and channels from the legacy LTE in terms of both DL and UL with of course some specific moderations.

2.2.1 DL Resource Grid:

The downlink framework of NB-IoT technology operates on the conventional Orthogonal Frequency Division Multiplexing (OFDM) waveform-based transmission system. In the frequency domain, the transmission bandwidth of 180 kHz span is granted within 12 subcarriers with 15 kHz spacing in between each subcarrier.

In the time domain, resource allocation depends upon a certain factor T_s, the period needed for sampling an OFDM symbol used in NB-IoT downlink. The factor goes by:

$T_s = 1/(\Delta f \times 2048) = 1/(15000 \times 2048)$ seconds $= 3.255\times10^{-8}$ seconds[21].

Based upon the factor T_s:

- Slot duration, $T_{slot} = (15360 \times T_s) = 0.5$ms
- Subframe duration, $T_{Subframe} = (30720 \times T_s) = 1$ms

- Radio Frame duration, $T_f = (307200 \times T_s) = 10ms$

As the downlink resource grid is mapped out in Fig. 1, each 10ms length Radio Frame consists of ten consecutive Subframes of 1ms each. Again, each 1ms subframe incorporates two consecutive slots of 0.5ms length. So, each radio frame comprises 20 slots in the downlink framework.

Within a radio frame, each slot is constituted with subsequent number of OFDM symbols and corresponding cyclic prefixes. In the downlink structure based on 15 kHz subcarrier spacing, seven OFDM symbols and their corresponding seven cyclic prefixes (CP) constitute a slot of 0.5ms length. According to Release 13[27], only one cyclic prefix (CP) is required to be transmitted along with corresponding OFDM symbol. The duration of single OFDM symbol for 15 kHz subcarrier spacing is, $T_{Symbol} = 1/\Delta f = 1/ 15000 = 66.67$ µs.

The length of the corresponding cyclic prefix (CP) goes by:

- $T_{CP} = (160 \times T_s) = 5.2$ µs, for OFDM symbol #0
- $T_{CP} = (145 \times T_s) = 4.7$ µs, for OFDM symbol #1- #6

For NB-IoT downlink structure, only QPSK modulation format is employed for necessary data transmission[28].

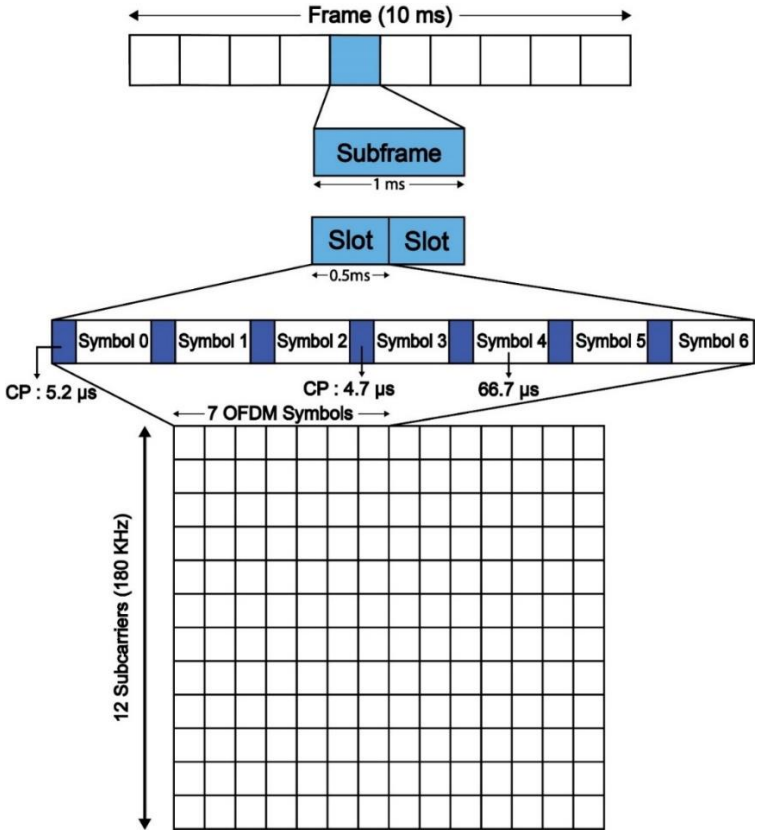

Figure 2.4: Downlink Resource Grid (with 15 kHz subcarrier spacing)

2.2.2 UL Resource Grid:

For the uplink data transmission, NB-IoT operates on Single-Carrier Frequency Division Multiple Access (SC-FDMA) waveform-based technique[23]. Two different schemes are accessible for the uplink data transmission:

In the case of Single-tone transmission, there are two disparate numerologies accessible in terms subcarrier spacing variation in the frequency domain[29]:

i. 15 kHz subcarrier spacing

ii. 3.75 kHz subcarrier spacing

In the case of Multi-tone transmission, system is operated solely based on 15 kHz subcarrier spacing. The frame structure, outlined in Fig: 2 for both Single-tone transmission and Multi-tone transmission with 15 kHz subcarrier spacing, follows the same parameters available for the NB-IoT downlink transmission, with 12 subcarriers within 180 kHz transmission bandwidth in the frequency domain and a 10ms radio frame comprising 20 slots with seven SC-FDMA symbols in each slot in the time domain. As for the Multi-tone transmission, considering different circumstances, these 12 subcarriers can even be employed as a group of subcarriers where 3, 6 and even 12 consecutive subcarriers can be stacked together to meet the data transmission requirement[30].

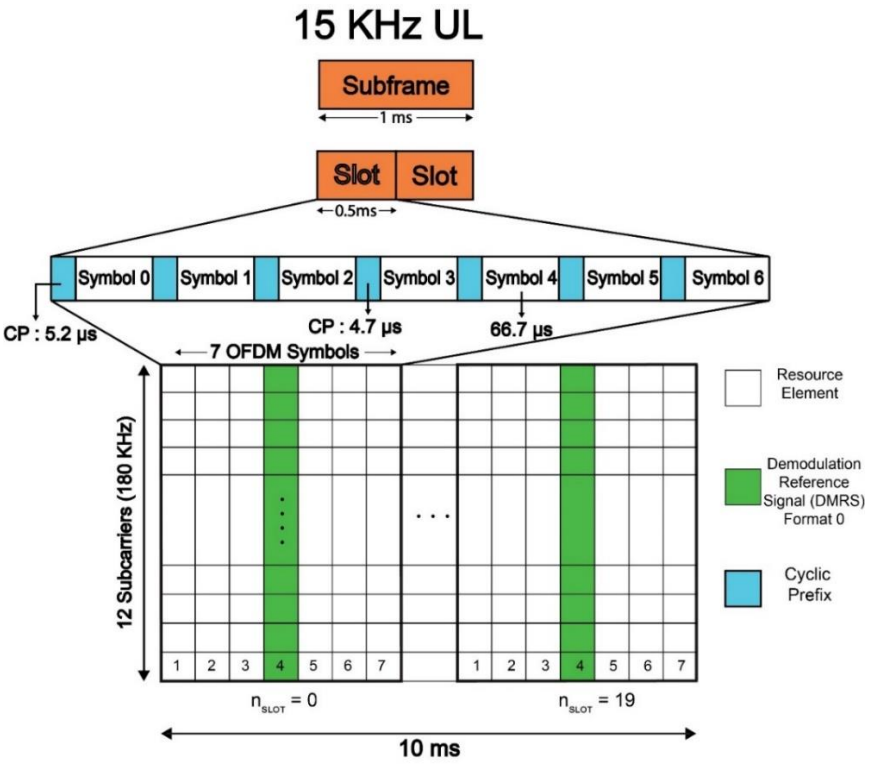

Figure 2.5: Uplink Resource Grid (with 15 kHz subcarrier spacing)

Nevertheless, the frame structure for resource allocation based on 3.75 kHz subcarrier spacing has been quite modified from the previous resource grid based on 15 kHz subcarrier spacing. As it is delineated in Fig: 3, in the frequency domain, the transmission bandwidth of 180 kHz span is allocated within 48 subcarriers with 3.75 kHz spacing in between each subcarrier.

In the time domain, the factor T_s, the time required for sampling an SC-FDMA symbol used in NB-IoT uplink, goes by:

$T_s = 1/(\Delta f \times 2048) = 1/(3750 \times 8192)$ seconds $= 3.255 \times 10^{-8}$ seconds.

For the abovementioned scheme, based on the factor T_s:

- Slot duration, $T_{slot} = (61440 \times T_s) = 2$ms
- Radio Frame duration, $T_f = (307200 \times T_s) = 10$ms

So, a 10ms radio frame comprises 5 slots in the uplink resource grid of 3.75 kHz subcarrier spacing. Each 2ms slot is constituted with seven SC-FDMA symbols and their corresponding seven cyclic prefixes (CP) and a guard period (GP) at the end of each slot. The duration of single SC-FDMA symbol for 3.75 kHz subcarrier spacing is,

$T_{Symbol} = 1/\Delta f = 1/ 3750 = 266.67$ µs.

Based on the factor T_s for 3.75 kHz subcarrier spacing, the length of the corresponding cyclic prefix (CP) and guard period (GP) go by:

- $T_{CP} = (255 \times T_s) = 8.3$ µs
- $T_{GP} = (2304 \times T_s) = 75$ µs

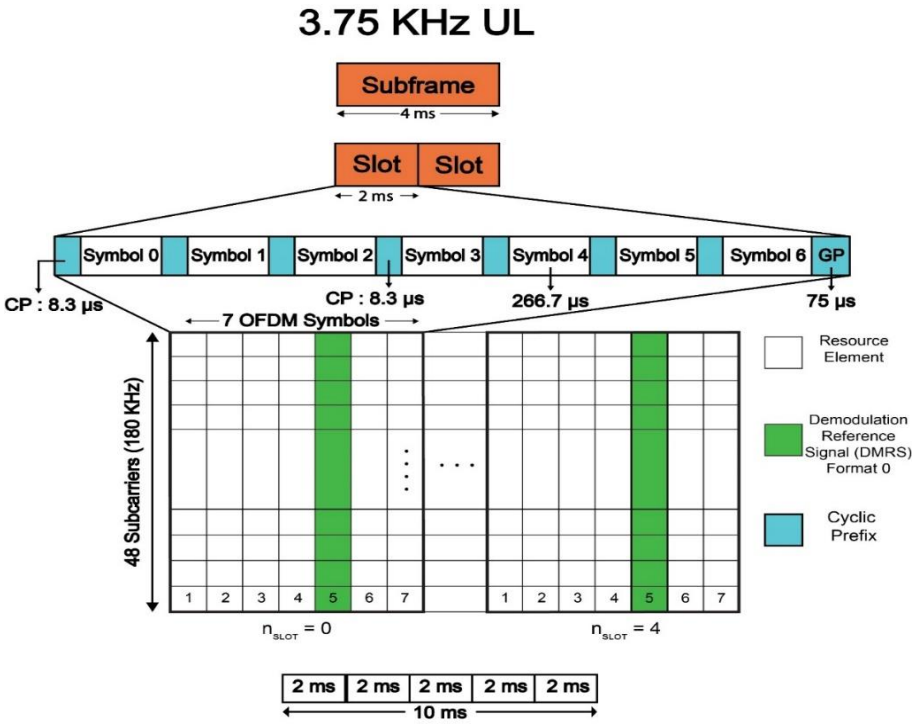

Figure 2.6: Uplink Resource Grid (with 3.75 kHz subcarrier spacing)

An exclusive feature has been added, by 3GPP in [31], in the NB-IoT uplink transmission system specified as Resource Unit (RU), mainly amalgamating discrete subcarriers and slots in frequency and time domain, respectively.

For single-tone uplink, a resource unit (RU) can be allocated as:

i. 16 slots (8ms) in case of 15 kHz subcarrier
ii. 16 slots (32ms) in case of 3.75 kHz subcarrier

For multi-tone uplink, using 15 kHz subcarrier only, a resource unit (RU) can be allocated as:

i. 3 subcarriers (4ms)
ii. 6 subcarriers (2ms)
iii. 12 subcarriers (1ms)

In the case of ACK/NACK transmission in uplink, a resource unit (RU) can be allocated as[23]:

i. 2ms, single subcarrier for 15 kHz
ii. 8ms, single subcarrier for 3.75 kHz

Two different modulation techniques have been designated for NB-IoT uplink data transmission:

i. $\pi/4$-QPSK and $\pi/2$-BPSK, in the case of single-tone transmission
ii. QPSK, in the case of multi-tone transmission

2.3 DL Physical Channels and Signals:

In the NB-IoT downlink framework, data transmission system is governed by some specific physical channels and signal.

The available three downlink physical channels and four signals are discussed in the following sections.

2.3.1 NPSS & NSSS:

To perform certain elementary actions like conducting nearby cell detection, time and frequency synchronicity, the Narrowband Synchronization Signals, namely NPSS and NSSS, are required for initial downlink data transmission.

NPSS is transmitted[32]:

- In subframe #5 of every radio frame with 10ms periodicity
- In OFDM symbol no. #3 to #13 and subcarrier no. #0 to #10

NSSS is transmitted[32]:

- In subframe #9 of every radio frame with 20ms periodicity
- In OFDM symbol no. #3 to #13 and subcarrier no. #0 to #11

2.3.2 NRS:

To perform channel estimation in the frequency domain, NRS is required for the downlink transmission. It is also known as “pilot” signal. NRS is generally transmitted:

- In the OFDM symbol no. #5, #6, #12 and #13 and subcarrier no. #0 to #11

NRS is restricted from transmission in those specific subframes allocated for either NPSS or NSSS[33].

Additionally, CRS is transmitted in the downlink channel using the same subframes allocated for NRS. Moreover, if the specific subframe available for CSR coincides with the same subframe allocated for NPSS and NSSS, CRS has the capability to puncture NPSS or NSSS and ensure proper transmission[23].

2.3.3 NPRS:

First arrived in the 3GPP Release 14[31], NPRS to employed to provide finer positioning assistance for NB-IoT devices. Using this feature, UEs can efficiently compute their position and notify the corresponding eNodeBs’ without using extravagant GPS services currently [34].

2.3.4 NPBCH:

The Narrowband master Information Block (MIB-NB) is transported through the Broadcast Channel (BCH) mapped into the NPBCH in the NB-IoT downlink transmission system. NPBCH is generally transmitted:

- In subframe #0 of every radio frame with 10ms periodicity
- In OFDM symbol no. #3 to #13 and subcarrier no. #0 to #11, the OFDM symbol no. #0, #1 and #2 are abstained from allocation for NPBCH to avoid probable collisions with LTE channels and the REs engaged for signals like CRS of LTE and NRS of NB-IoT[34].

While data transfer, NPBCH utilizes the QPSK modulation scheme[22].

2.3.5 NPDCCH:

To transmit the essential control information and scheduling instructions for both downlink and uplink system, NPDCCH is employed. While transmission, NPDCCH utilizes the QPSK modulation scheme. It is allocated in all the available subframes in the downlink resource grid, ostracizing the specific subframes required for NPBCH, NPSS and NSSS[34]. It implies

two levels of Narrowband Control Channel Elements (NCCE) and three DCI formats during transmission procedure[22].

2.3.6 NPDSCH:

To transfer downlink user data, System Information Block (SIB), Random Access Response (RAR) messages and paging messages, NPDSCH is employed in downlink transmission system[32]. Similar to NPDCCH, while transmission, NPDCCH utilizes the QPSK modulation scheme. It is allocated in all the available subframes in the downlink resource grid, ostracizing the specific subframes no. #0, #5 and #9 which are required for NPBCH, NPSS and NSSS transmission[34].

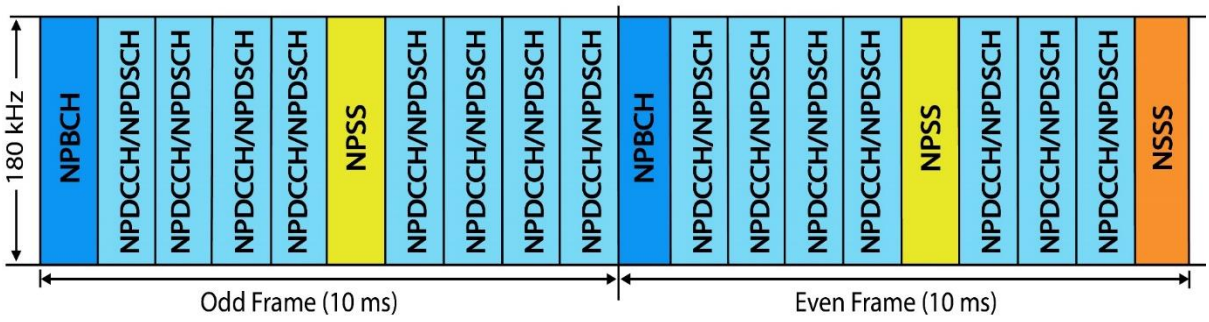

Figure 2.7: Downlink Resource Scheduling (with 15 kHz subcarrier spacing)

2.4 UL Physical Channels and Signals:

In the NB-IoT uplink framework, data transmission system is controlled by two different physical channels and single signal, discussed in the following sections.

2.4.1 NPRACH:

To fabricate a rudimentary interconnection between eNodeB and UE, the NPRACH is employed. NPRACH utilizes the Random Access Response (RAR) procedure to ensure the initial bridge in between base station and NB-IoT devices[22]. Each NPRACH preamble has a frame of 4 symbol groups with 5 symbols and a cyclic prefix (CP). Each symbol is transferred utilizing 3.75 kHz subcarrier along with a span of 266.7 µs in the time domain. Considering the variation in cell radius, CP length can be deployed as[35]:

- Format 0, implying CP length of 66.67 µs (up to 10 km)
- Format 1, implying CP length of 266.7 µs (up to 40 km)

In the frequency domain, to mollify the chance of collision among signals transmitted from various UEs residing closed by, the frequency hopping technique is applied, and thus NPRACH inhabits a contiguous set of subcarriers, either 12,24,36 or 48 [36]. To improve the probability of signal reception, repetition of 1, 2, 4, 8, 16, 32 and 64 times of the NPRACH preamble is allowed [22].

2.4.2 NPUSCH:

To transmit both control and data information from the UE side, the NPUSCH is employed in the uplink transmission system. During the NPUSCH transmission process, two different formats are being used[34]:

- Format 1, carrying Data information
- Format 2, carrying Control information

According to data transmission requirement, more than one RU can be dedicated to NPUSCH at times[37].

2.4.3 DMRS:

In the frequency domain, to speculate the channel condition from the UE side, the DMRS is employed[34]. Its resource allocation depends on the same Resource Units (RU) chartered for NPUSCH.

- In the case of NPUSCH format 1, it can be transmitted in the SC-FDMA symbol no. #3 and #4 corresponding to 15 kHz and 3.75 kHz subcarrier spacing, respectively.
- In the case of NPUSCH format 2, it can be transmitted in the set of symbols #2, #3, #4, and #0, #1, #2 corresponding to 15 kHz and 3.75 kHz subcarrier spacing, respectively [23].

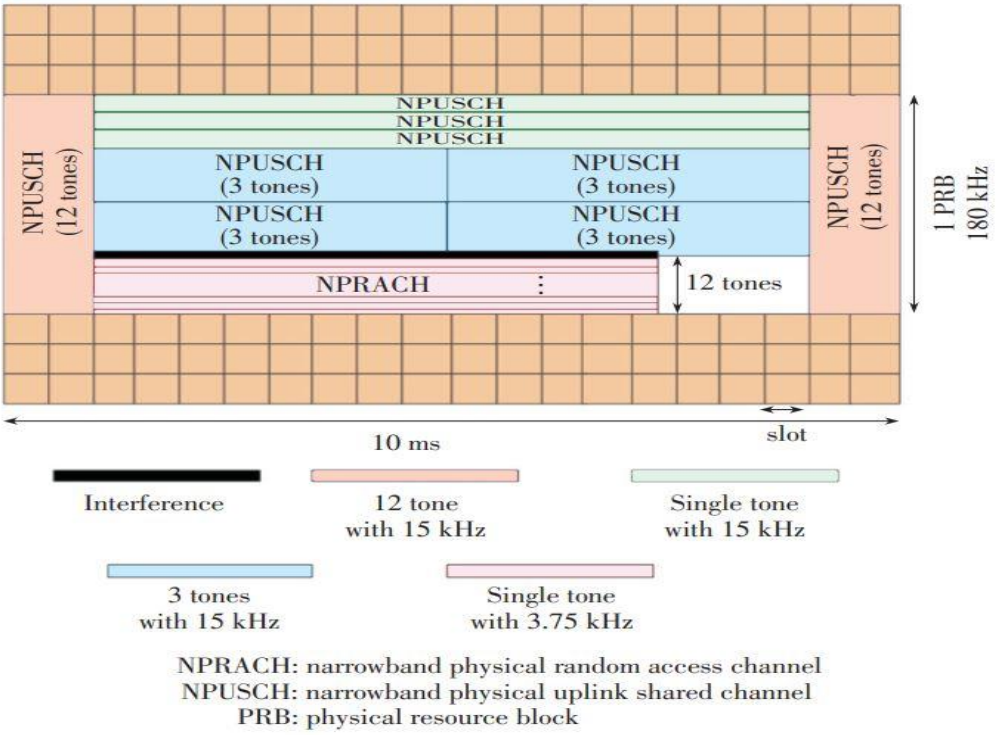

Figure 2.8: Uplink Resource Scheduling (In-band Mode)[38]

Chapter 3

Methodology

In this era of ubiquitous connectivity among all the devices, some software-driven NB-IoT devices operate on a system with periodic uplink transmission of short messages on regular intervals. The aforementioned short message system-based transmission generally does not enact any stringent latency requirements and can operate with even minimum data rate requirement. For uplink transmission, each device is allocated with one RU as per requirement [37]. For this scenario, a modified resource grid with an increment in the number of subcarriers can offer an increment in the number of connected devices each for single-tone uplink transmission.

In this thesis, for the abovementioned scenario, taking into account some specific design consideration, a modified resource grid with an increment in the number of subcarriers has been proposed that offers an increment in the number of connected devices for single-tone uplink transmission, and also the performance of the proposed 1.875 kHz subcarrier spacing has been thoroughly investigated under different scenarios with substantial simulations.

3.1 Design Considerations

The following factors should be kept in mind while modifying the existing resource grid for uplink to increase the number of connected devices with due efficiency:

3.1.1 DMRS Positioning:

While positioning the Demodulation Reference Signal (DMRS) in the modified resource grid, the transmission of LTE Sounding Reference Signal (SRS) has to be taken into account during the In-band mode operation. Generally, LTE SRS is transmitted in the very last symbol of a subframe, as per requirement. As visualized in Fig: 4, there lies a possibility that LTE SRS may collide with the even numbered symbols of a NB-IoT subframe. If DMRS is positioned in one of those even numbered symbols, there lies strong probability that LTE SRS may puncture DMRS and cause total disruption in NB-IoT channel[39]. So DMRS should only be allocated in either of the odd numbered symbols in a NB-IoT subframe.

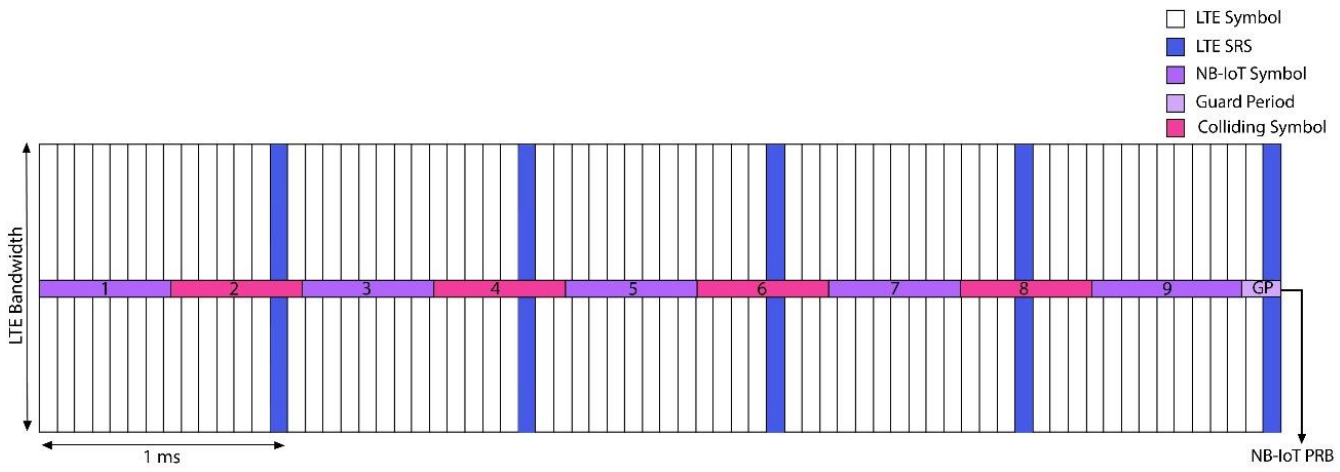

Figure 3.1: Data/DMRS symbol arrangement in scaled slot/subframe for 1.875 kHz subcarrier spacing

3.1.2 Length of CP:

An increment in the length of cyclic prefix (CP) can offer some advantages:

- It becomes easier to detect NPRACH even from UE residing at poor coverage area.
- It acts as safety net in multipath environment from the disturbance the Inter-Symbol-Interference (ISI) can produce to spreading of a signal over time.

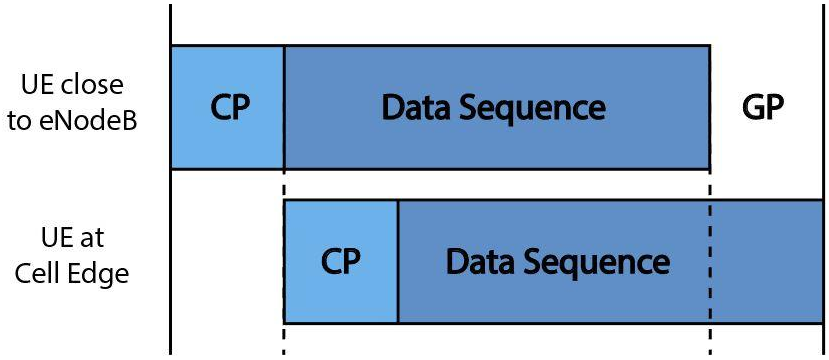

Figure 3.2: Cyclic Prefix/ Guard Period Dimension

3.1.3 Presence of GP:

The presence of a guard period (GP) at the end of each slot can provide advantages like:

- Mitigating the probability of havoc caused by possible ISI.
- Providing benefits while avoiding probable collision with LTE SRS, without losing much of transmission efficiency.

3.2 Proposed Scheme:

Taking all the design consideration into account, a new frame structure with 1.875 kHz subcarrier spacing and 5ms length slot conveying nine SC-FDMA symbols has been preferred. 1.875 kHz subcarrier spacing in the 180 kHz transmission bandwidth can accommodate 96 subcarriers in the frequency domain.

In the time domain, considering a factor representing necessary period for sampling an SC-FDMA symbol used in the proposed scheme with 1.875 kHz subcarrier spacing, T_s = 1/(16384 × 1875) seconds = 3.255×10^{-8} seconds, the available parameters:

- Slot duration, T_{slot} = (153600 × T_s) = 5ms
- Subframe duration, $T_{Subframe}$ = (307200 × T_s) = 10ms

Thus, a radio frame holds two slots. Each slot contains nine SC-FDMA symbols, each of, T_{symbol} = 1/Δf = 1/ 1875 = 533.4 µs length.

Based on the factor T_s, length of the following parameters:

- T_{CP} = (418 × T_s) seconds = 13.6 µs
- T_{GP} = (2304 × T_s) seconds = 75 µs length

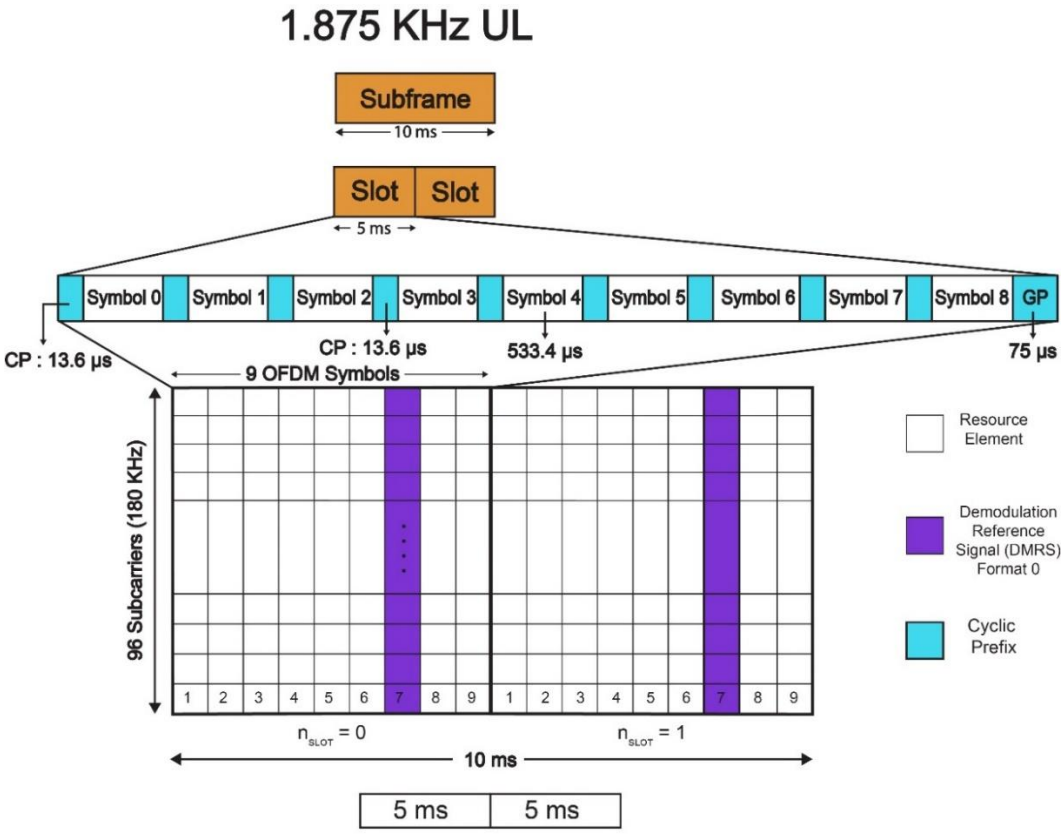

Figure 3.3: Proposed Uplink resource Grid (with 1.875 kHz Subcarrier Spacing)

To avoid probable collision mentioned above, DMRS has been allocated in the symbol no. #6 in the NB-IoT uplink framework.

Chapter 4

Software based Performance Testing

Rigorous software based testing has been done regarding the NB-IoT link level scenarios using both the already existing and our newly proposed subcarrier spacings. The simulations have been done for all three of the deployment modes: standalone, Guard-band and in-band modes. They provide us with the following results:

Bit Error Rate (BER): The percentage of bits altered during transmission through a channel relative to total bits transmitted is called Bit Error Rate. Bits can get altered due to many reasons such as distortion, interference, noise, bit synchronization error etc. It is a PHY layer property. Increasing SNR and decreasing pathloss increases BER.

Frame Error Rate (FER): A single bit error in an entire frame counts as a frame error. The percentage of frames having error during transmission through a channel relative to total frames transmitted is called Frame Error Rate. It is a Data Link Layer (DLL) property. Increasing SNR and decreasing pathloss increases FER.

Throughput: Throughput is the number of bits transmitted in one second. It can vary due to latency, packet loss, jitters etc. Increasing SNR and decreasing pathloss increases throughput.

Channel Estimation Error (CEE): Channel estimation helps to make throughput more efficient. Channel quality continuously varies. It can be done by pilot sequence. The calculation in our simulation has been done by MMSE. Knowing channel and noise distribution can allow us to reduce channel error. Increasing SNR and decreasing pathloss increases channel error.

Peak to Average Power Ratio (PAPR): A signal has a maximum power and an average power. The ratio between them is called Peak to Average Power Ratio. Different subcarriers that are out of phase from each other cause PAPR. In OFDM, the peak can be very high as the subcarriers are modulated independently. PAPR helps in choosing the Power Amplifier (PA) of a system. The lower the PAPR, the better. Because, PA is the most power consuming unit in a base station. Thus, PAPR reduction increases PA efficiency. We use PAPR to set the

average power just low enough to minimize clipping. In wireless link, the PAPR of the signal is a statistical quantity. The probability of a given peak power helps decide where to set the average power level of the PA.

4.1 Standalone Deployment:

Standalone mode is used when there is no other cellular service present. This is done by using the cellular spectrum that was previously used by GSM. The GSM carriers are reframed into NB-IoT subcarriers.

Some of the available standalone bands for NB-IoT are:

NB-IoT Band	Uplink Band	Downlink Band	Bandwidth	Duplex Mode
B2	1850 - 1910 MHz	1930 - 1990 MHz	60 MHz	HD-FDD
B3	1710 - 1785 MHz	1805 - 1880 MHz	75 MHz	HD-FDD
B5	824 - 849 MHz	869 - 894 MHz	25 MHz	HD-FDD
B8	880 - 915 MHz	925 - 960 MHz	25 MHz	HD-FDD
B12	699 - 716 MHz	729 - 746 MHz	17 MHz	HD-FDD
B31	452.5 - 457.5 MHz	462.5 - 467.5 MHz	5 MHz	HD-FDD

Table 4.1: Permitted GSM bands and their LTE equivalents for NB-IoT standalone deployment

For simulation, we have used the GSM-850 band, which is equivalent to LTE-B5.
Simulation standalone Center Frequency: 836.5MHz.

4.1.1 Standalone BER vs SNR:

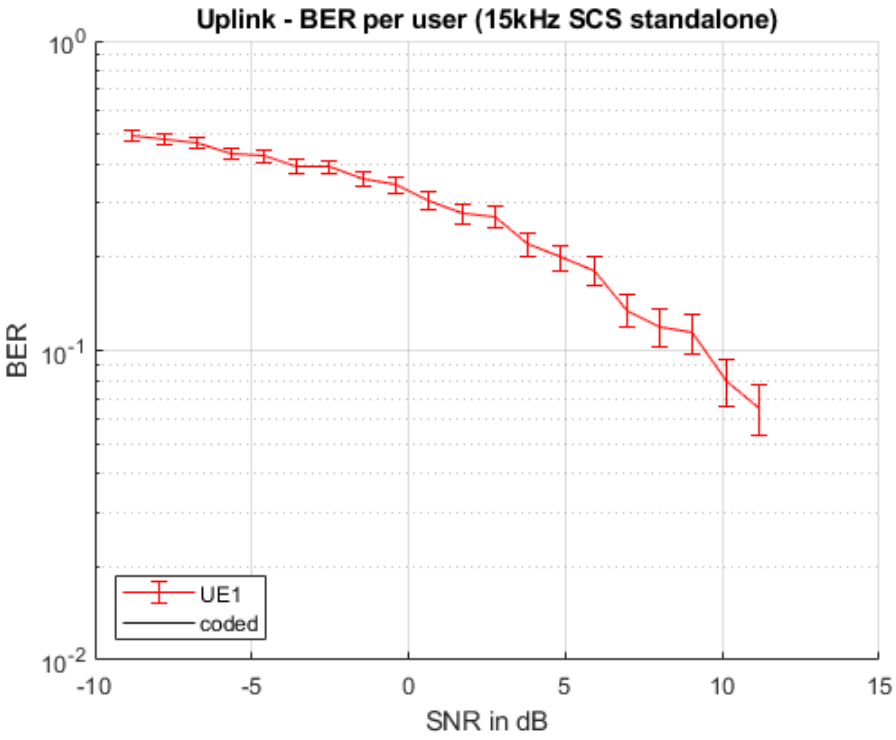

Fig 4.1: Already existing 15kHz SCS uplink BER in standalone mode

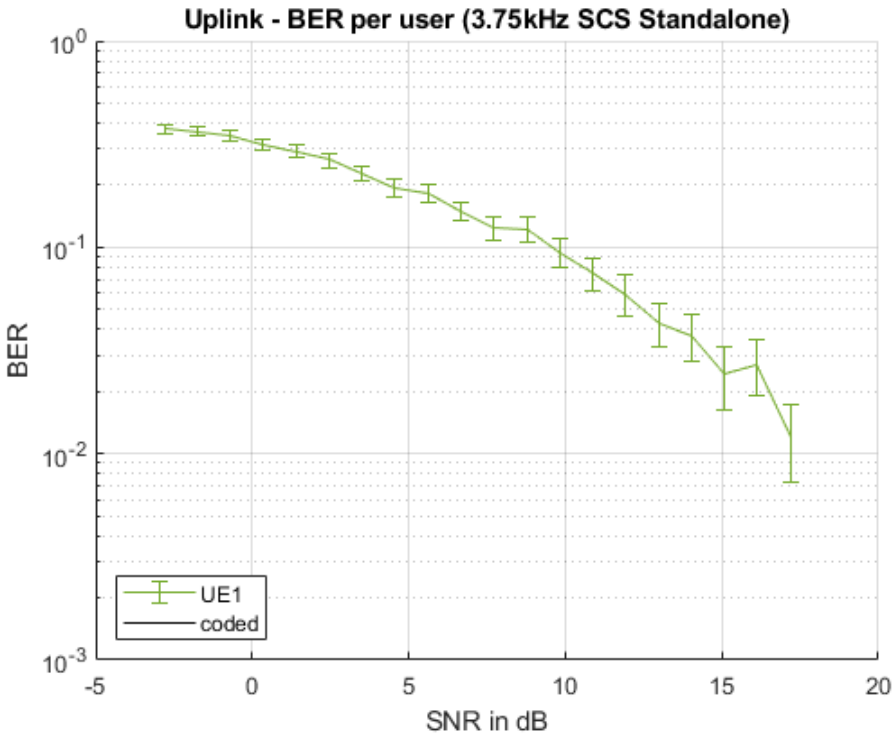

Fig 4.2: Already existing 3.75kHz SCS uplink BER in standalone mode

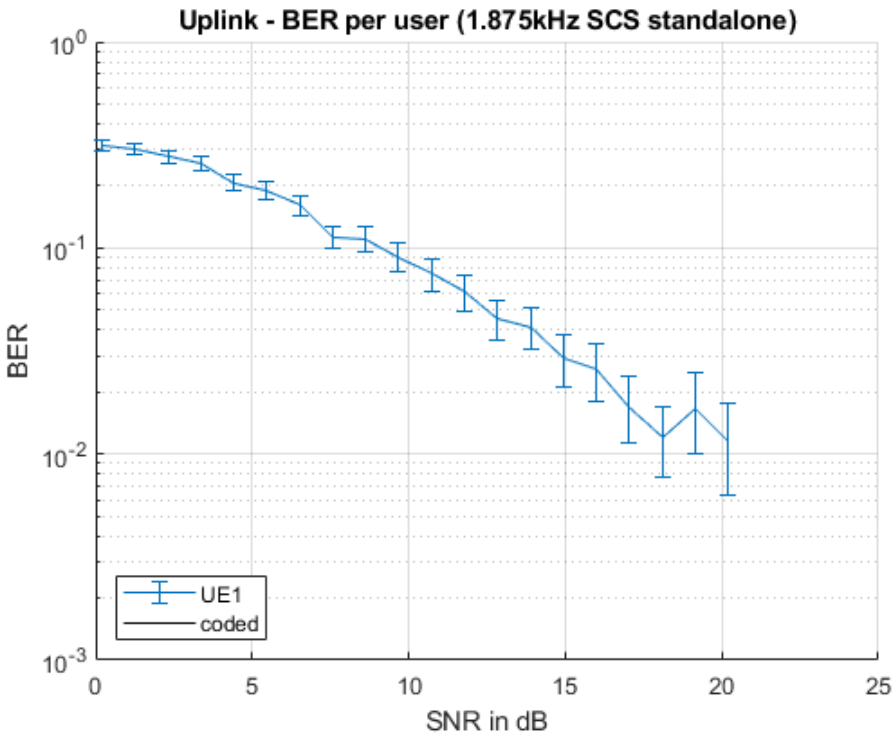

Fig 4.3: Our Proposed 1.875kHz SCS uplink BER in standalone mode

Result:

SCS \ SNR	0	5	10
15kHz	.34	.2	.08
3.75kHz	.32	.19	.09
1.875kHz	.3	.2	.085

Table 4.2: Standalone BER comparison

4.1.2 Standalone FER vs SNR:

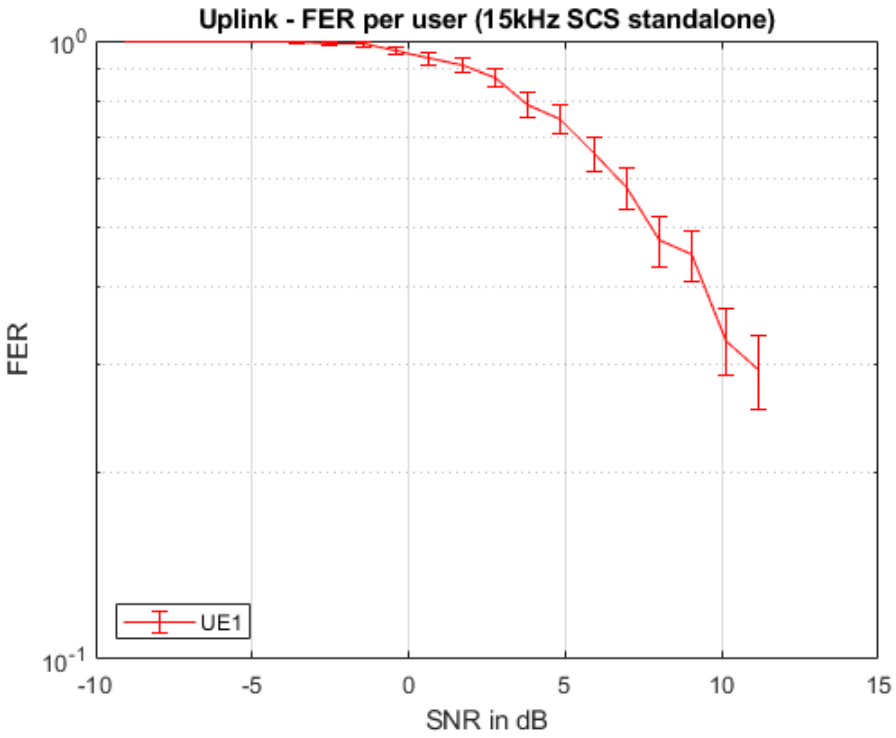

Fig 4.4: Already existing 15kHz SCS uplink FER in standalone mode

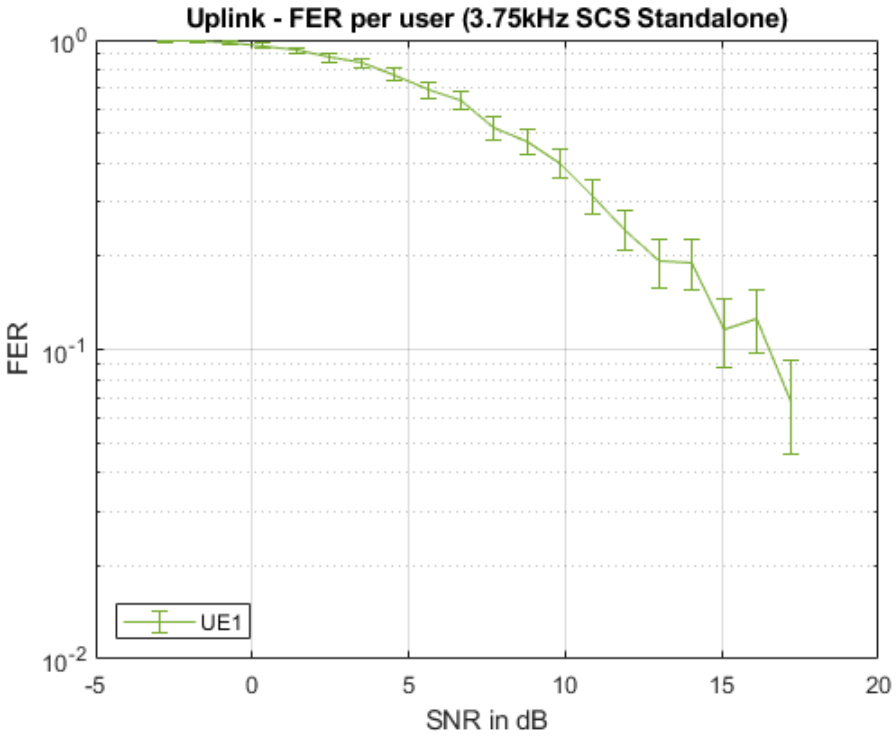

Fig 4.5: Already existing 3.75kHz SCS uplink FER in standalone mode

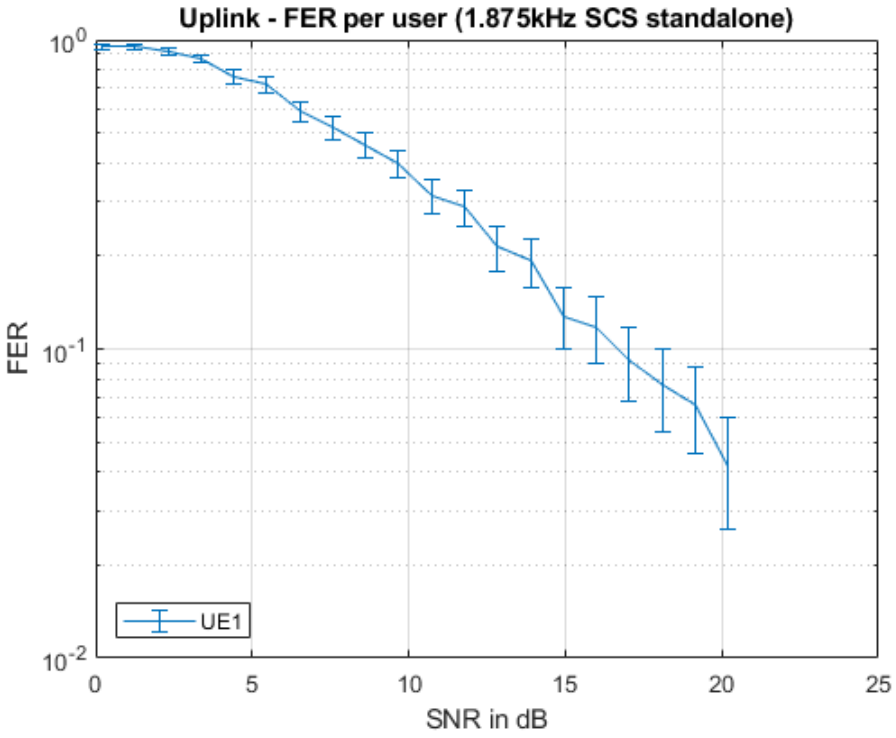

Fig 4.6: Our Proposed 1.875kHz SCS uplink FER in standalone mode

Result:

SCS \ SNR	0	5	10
15kHz	.95	.74	.24
3.75kHz	.93	.73	.13
1.875kHz	.9	.75	.15

Table 4.3: Standalone FER comparison

4.1.3 Standalone Throughput vs SNR:

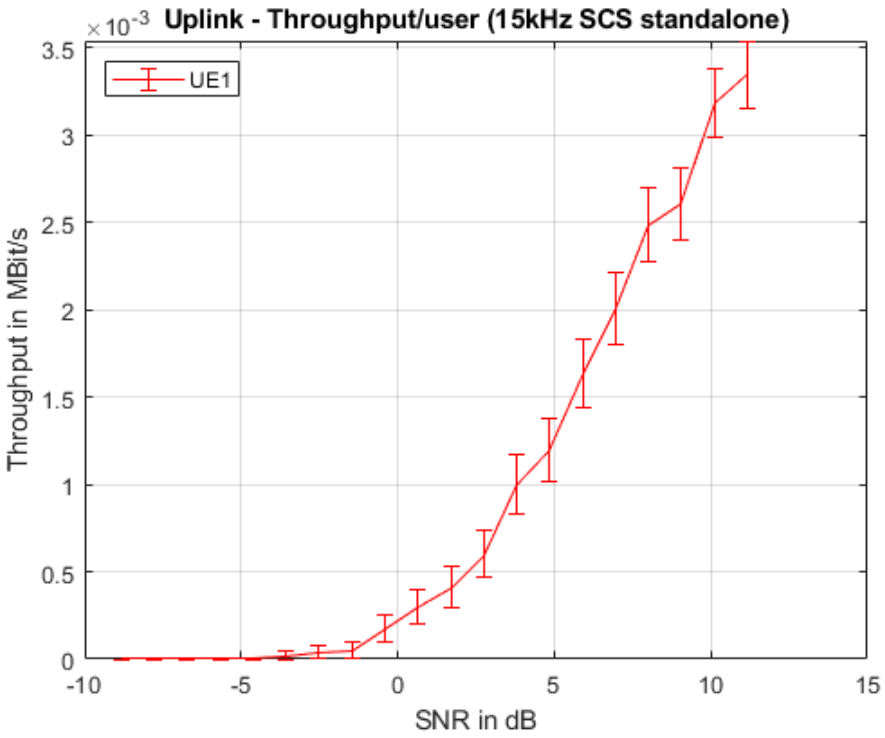

Fig 4.7: Already existing 15kHz SCS uplink throughput in standalone mode

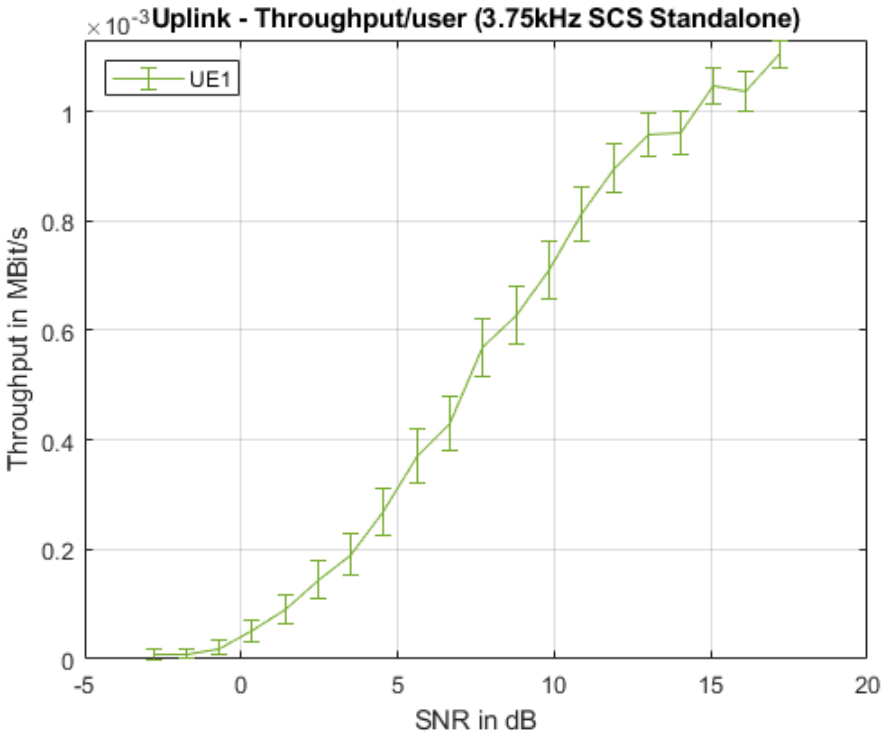

Fig 4.8: Already existing 3.75kHz SCS uplink throughput in standalone mode

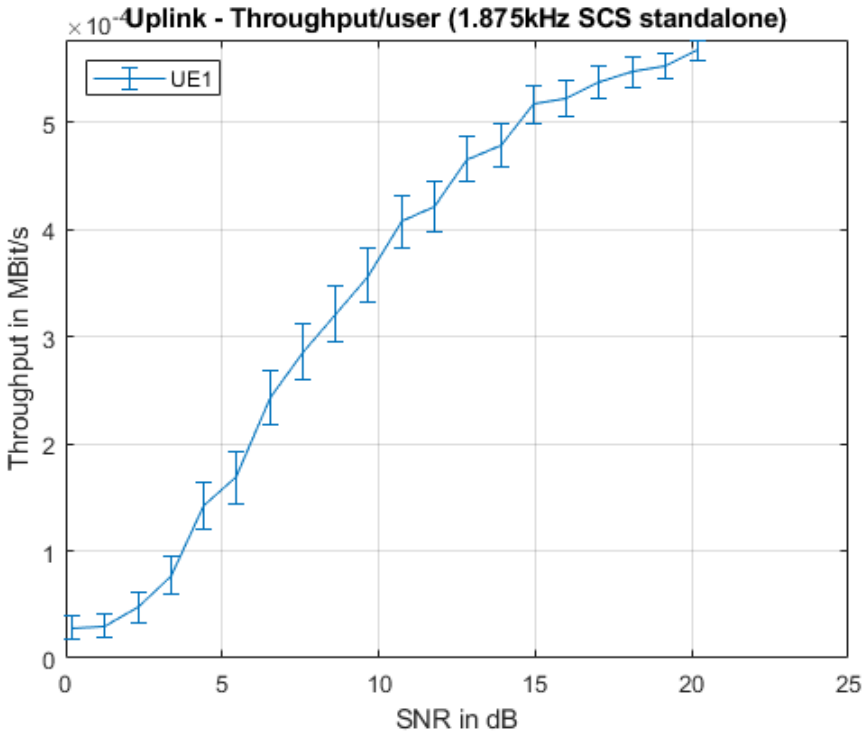

Fig 4.9: Our Proposed 1.875kHz SCS uplink throughput in standalone mode

Result:

SCS \ SNR	0	5	10
15kHz	0.2e-3	1.3e-3	3.2e-3
3.75kHz	.04e-3	.3e-3	.72e-3
1.875kHz	.3e-4	1.5e-4	3.8e-4

Table 4.4: Standalone throughput comparison

4.1.4 Standalone CEE vs SNR:

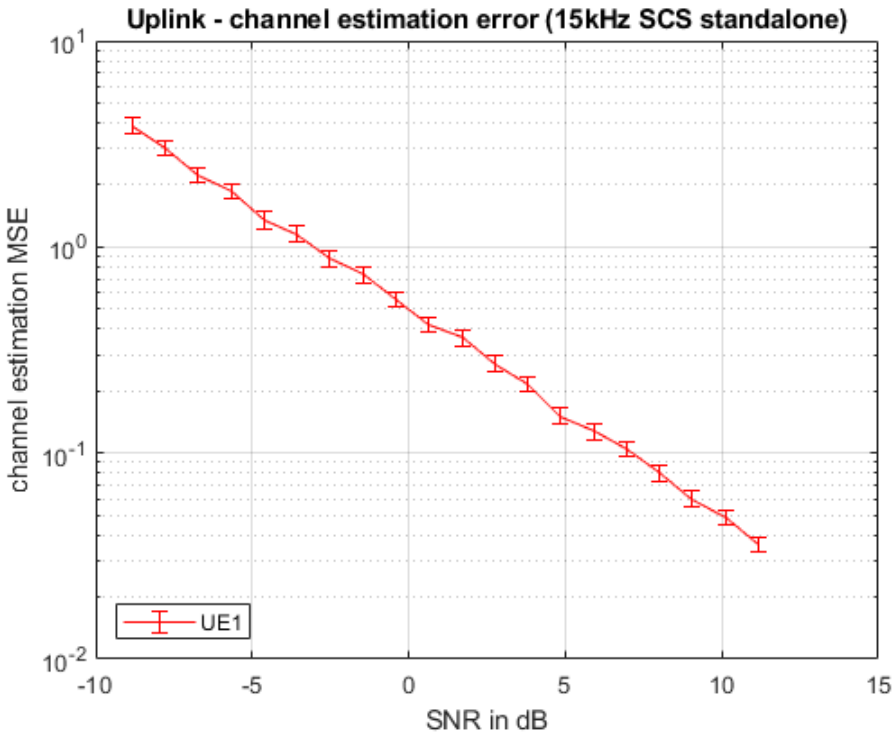

Fig 4.10: Already existing 15kHz SCS uplink CEE in standalone mode

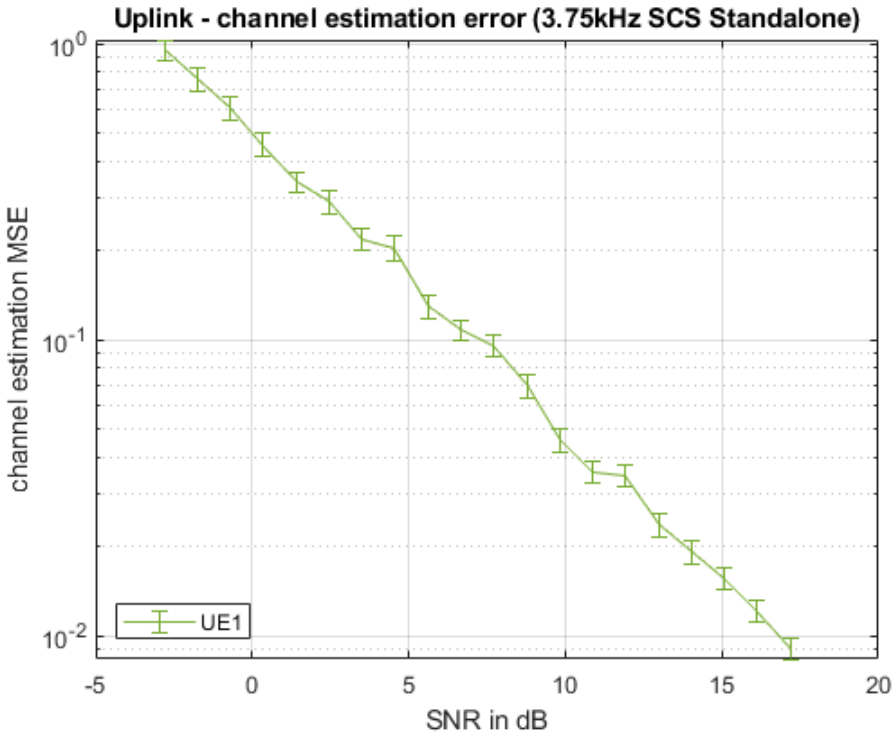

Fig 4.11: Already existing 3.75kHz SCS uplink CEE in standalone mode

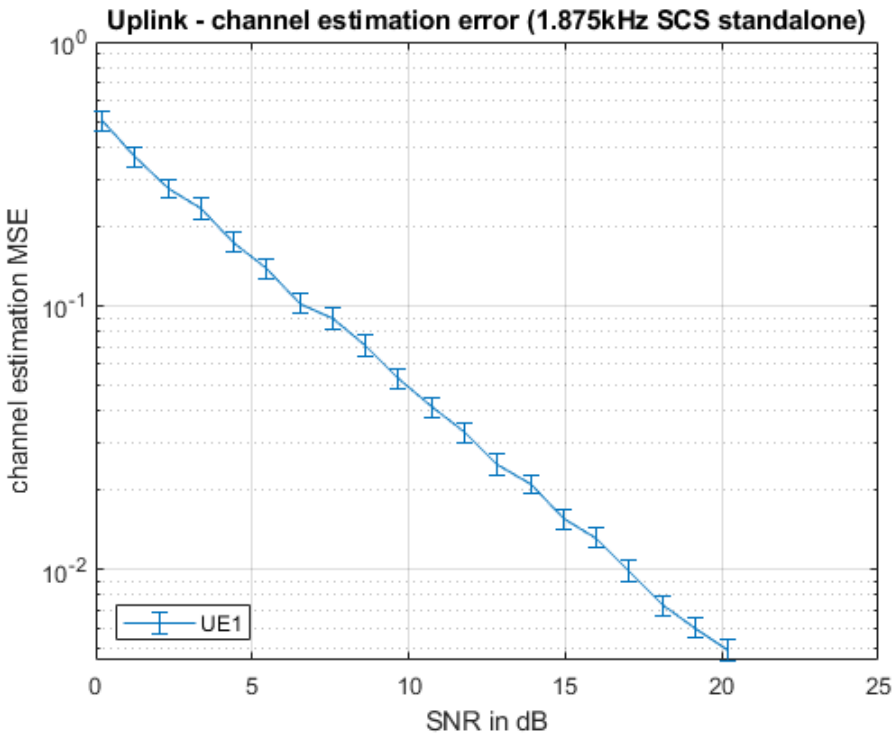

Fig 4.12: Our Proposed 1.875kHz SCS uplink CEE in standalone mode

Result:

SCS \ SNR	0	5	10
15kHz	.4	.15	.04
3.75kHz	.4	.17	.045
1.875kHz	.4	.16	.017

Table 4.5: Standalone CEE comparison

4.1.5 Standalone P vs PAPR:

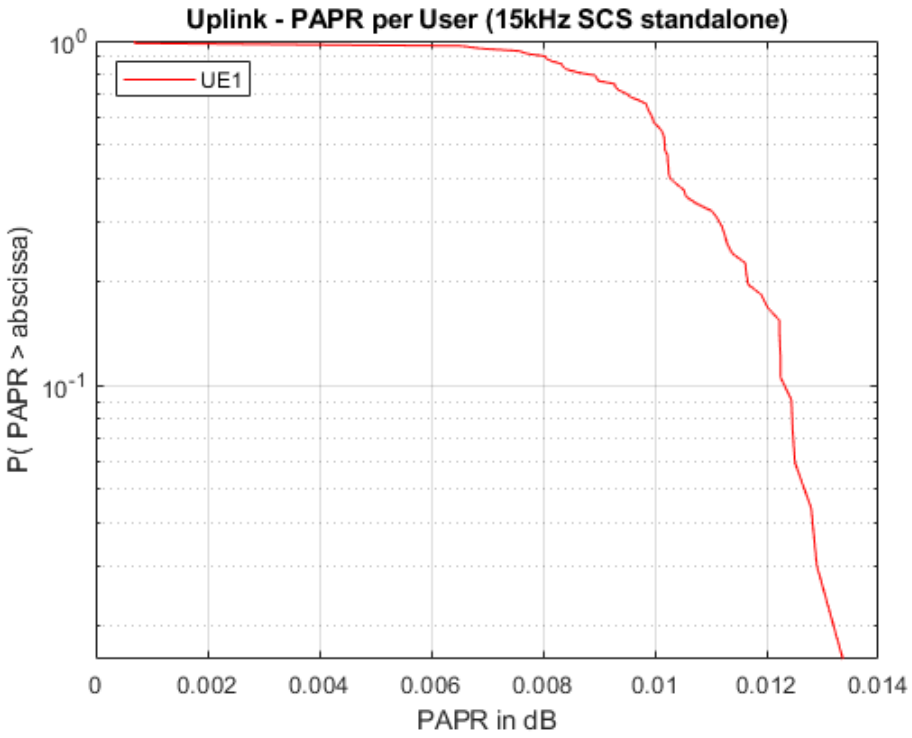

Fig 4.13: Already existing 15kHz SCS uplink PAPR in standalone mode

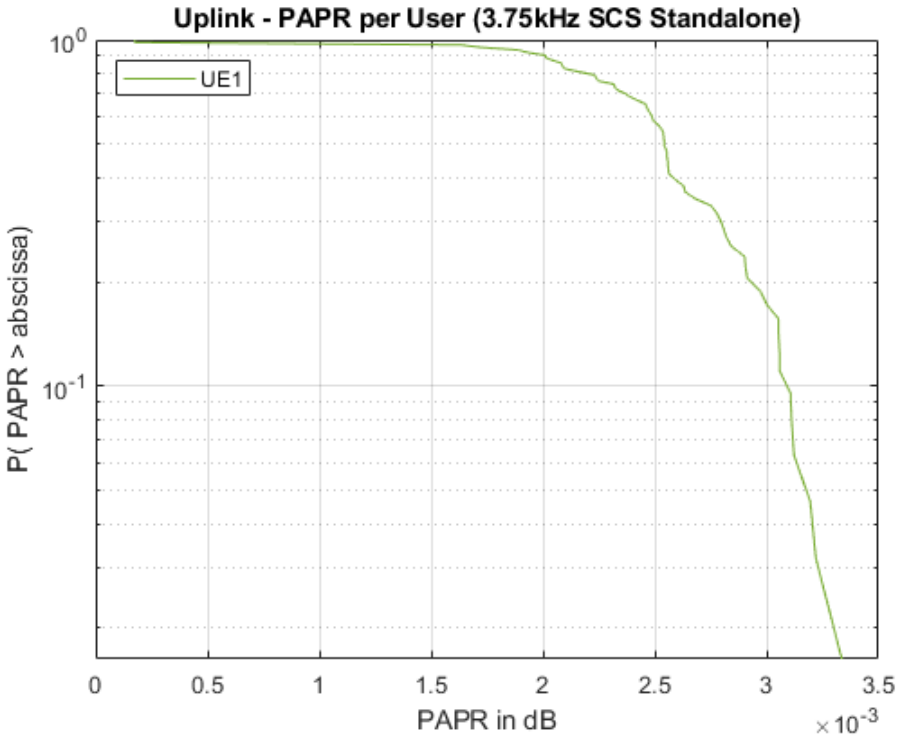

Fig 4.14: Already existing 3.75kHz SCS uplink PAPR in standalone mode

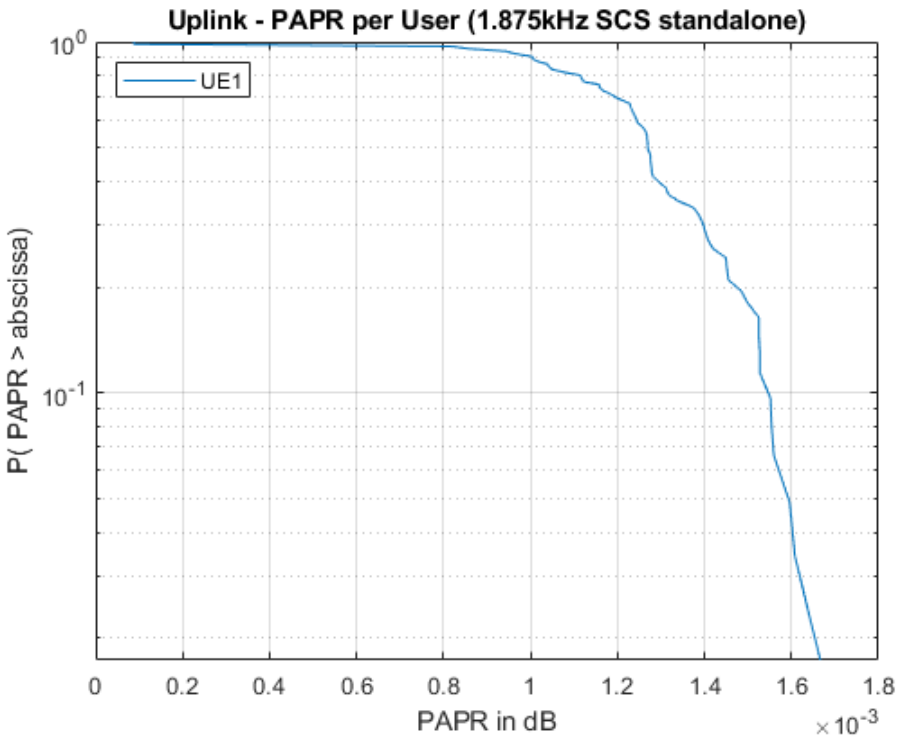

Fig 4.15: Our Proposed 1.875kHz SCS uplink PAPR in standalone mode

Result:

When PAPR is 1, PAPR in dB is 0. As PAPR is increasing, the probability CCDF function is decreasing. Thus, the probability of achieving the peak is decreasing.

P = 0.1 / SCS	At PAPR dB
15kHz	12.4e-3
3.75kHz	3.1e-3
1.875kHz	1.56e-3

Table 4.6: Standalone PAPR comparison

4.2 In-band Deployment

In-band mode is used when cellular service is present. The NB-IoT PRBs are positioned in the LTE carriers and they share the LTE resources. It is economically efficient. Also, the mobile operators can create the connection seamlessly and efficiently based on user device demand.

The in-band mode uses some permitted LTE bands. Some of the LTE bands permitted for NB-IoT are:

NB-IoT Band	Uplink Band	Downlink Band	Bandwidth	Duplex Mode
B1	1920 - 1980 MHz	2110 - 2170 MHz	60 MHz	HD-FDD
B2	1850 - 1910 MHz	1930 - 1990 MHz	60 MHz	HD-FDD
B3	1710 - 1785 MHz	1805 - 1880 MHz	75 MHz	HD-FDD
B4	1710 -1755 MHz	2110 -2155 MHz	45 MHz	HD-FDD
B5	824 - 849 MHz	869 - 894 MHz	25 MHz	HD-FDD
B8	880 - 915 MHz	925 - 960 MHz	25 MHz	HD-FDD
B11	1427.9 - 1447.9 MHz	1475.9 - 1495.9 MHz	20 MHz	HD-FDD
B12	699 - 716 MHz	729 - 746 MHz	17 MHz	HD-FDD
B13	777 - 787 MHz	746 - 756 MHz	10 MHz	HD-FDD
B14	788 - 798 MHz	758 to 768 MHz	10 MHz	HF-FDD
B17	704 - 716 MHz	734 - 746 MHz	12 MHz	HD-FDD

B18	815 - 830 MHz	860 - 875 MHz	15 MHz	HD-FDD
B19	830 - 845 MHz	875 - 890 MHz	15 MHz	HD-FDD
B20	832 - 862 MHz	791 - 821 MHz	30 MHz	HD-FDD
B25	1850 - 1915 MHz	1930 - 1995 MHz	65 MHz	HD-FDD
B26	814 - 849 MHz	859 - 894 MHz	35 MHz	HD-FDD
B28	703 - 748 MHz	758 - 803 MHz	45 MHz	HD-FDD
B31	452.5 - 457.5 MHz	462.5 - 467.5 MHz	5 MHz	HD-FDD
B66	1710 - 1780 MHz	2110 - 2200 MHz	70/90 MHz	HD-FDD
B70	1695 - 1710 MHz	1995 - 2020 MHz	25 MHz	HD-FDD
B71	633 - 698 MHz	617 - 783 MHz	65 MHz	HD-FDD
B72	451 - 456 MHz	461 - 466 MHz	5 MHz	HD-FDD
B73	450 - 455 MHz	461 - 466 MHz	5 MHz	HD-FDD
B74	1427 - 1470 MHz	1475 - 1518 MHz	43 MHz	HD-FDD
B85	698 - 716 MHz	728 - 746 MHz	10 MHz	HD-FDD

Table 4.7: Permitted LTE bands for NB-IoT guard/in-band deployment

For simulation, we have used the LTE-B1 band.

Simulation In-band Center Frequency:1950MHz.

4.2.1 In-band BER vs SNR:

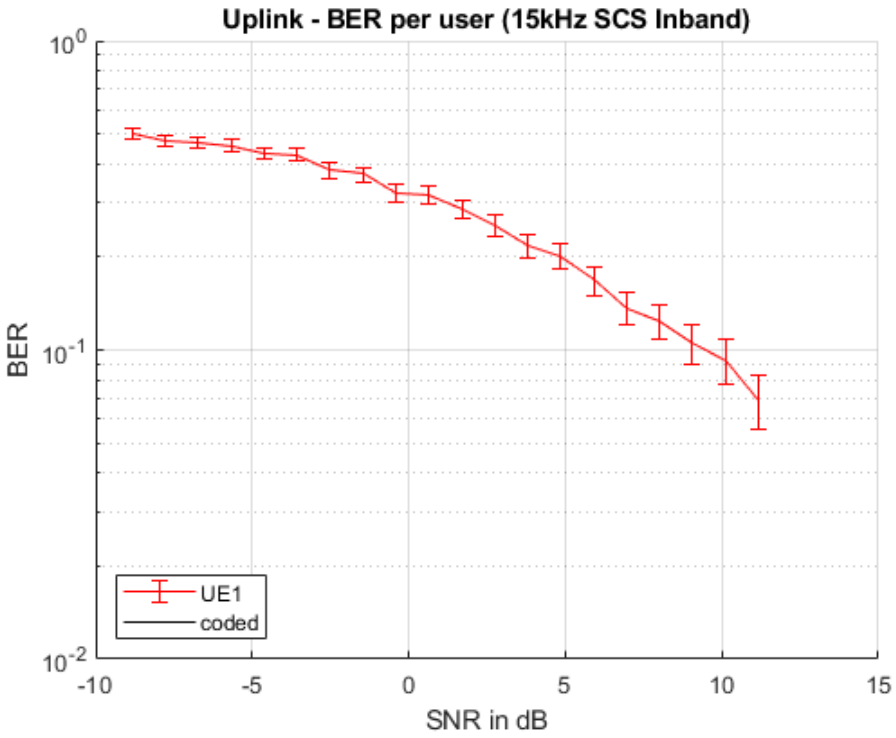

Fig 4.16: Already existing 15kHz SCS uplink BER in in-band mode

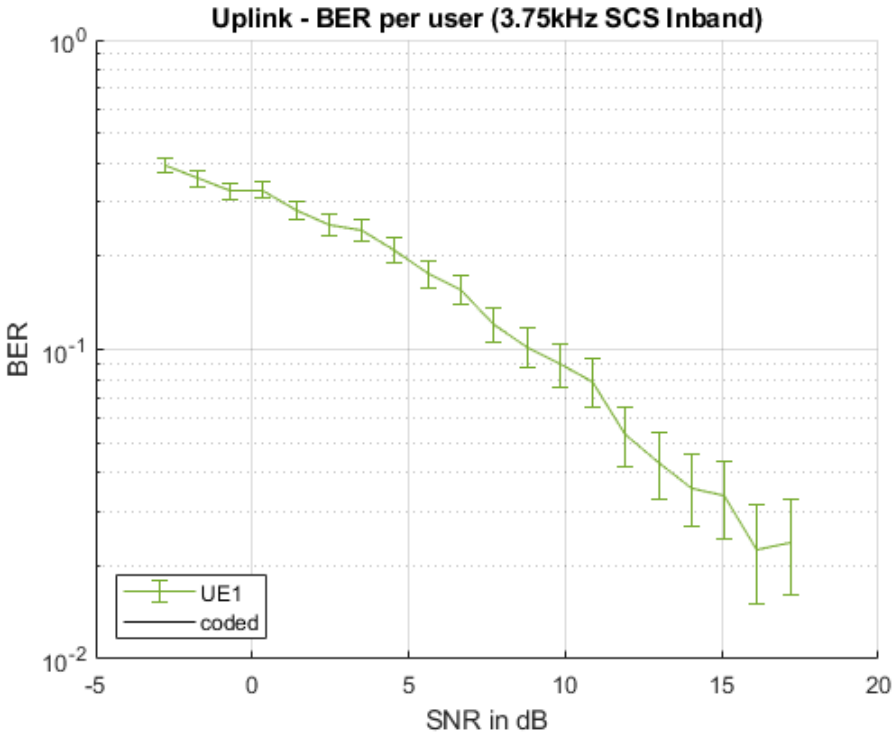

Fig 4.17: Already existing 3.75kHz SCS uplink BER in in-band mode

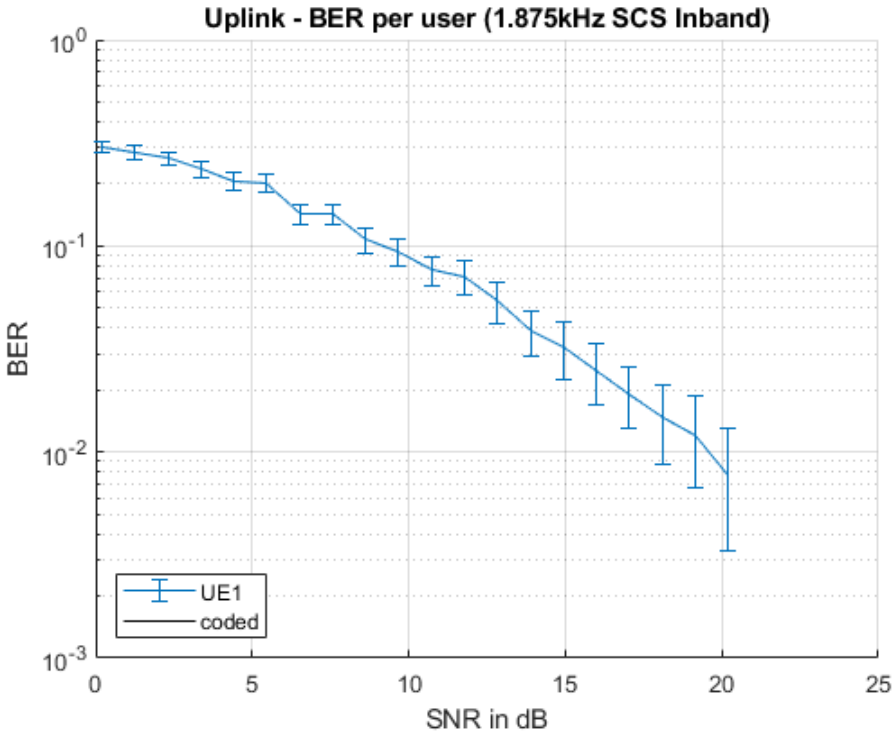

Fig 4.18: Our Proposed 1.875kHz SCS uplink BER in in-band mode

Result:

SCS \ SNR	0	5	10
15kHz	.33	.19	.093
3.75kHz	.33	.19	.035
1.875kHz	.3	.2	.09

Table 4.8: In-band BER comparison

4.2.2 In-band FER vs SNR:

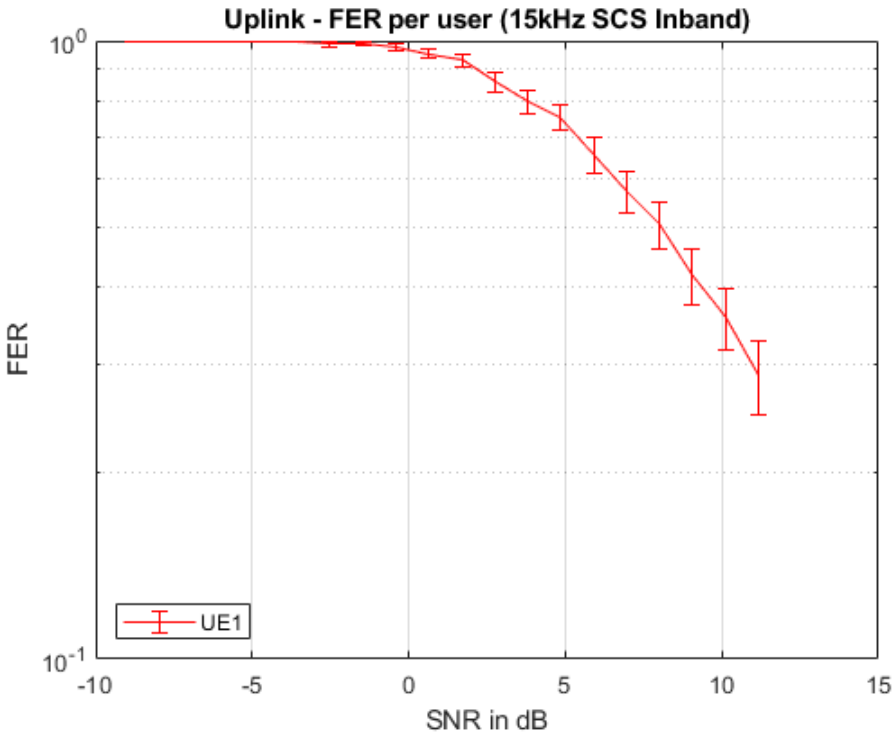

Fig 4.19: Already existing 15kHz SCS uplink FER in in-band mode

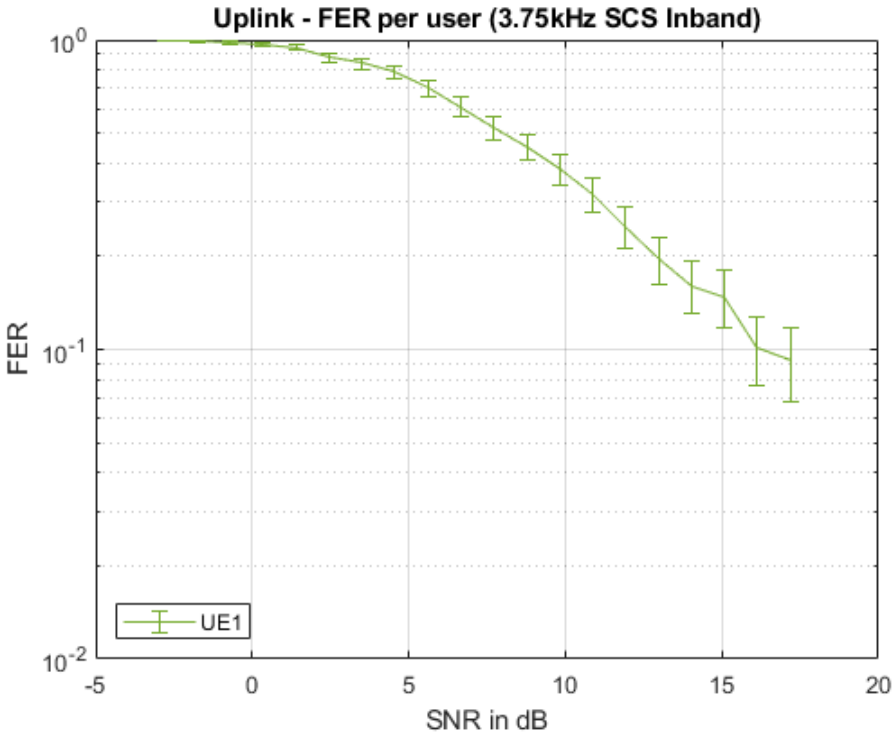

Fig 4.20: Already existing 3.75kHz SCS uplink FER in in-band mode

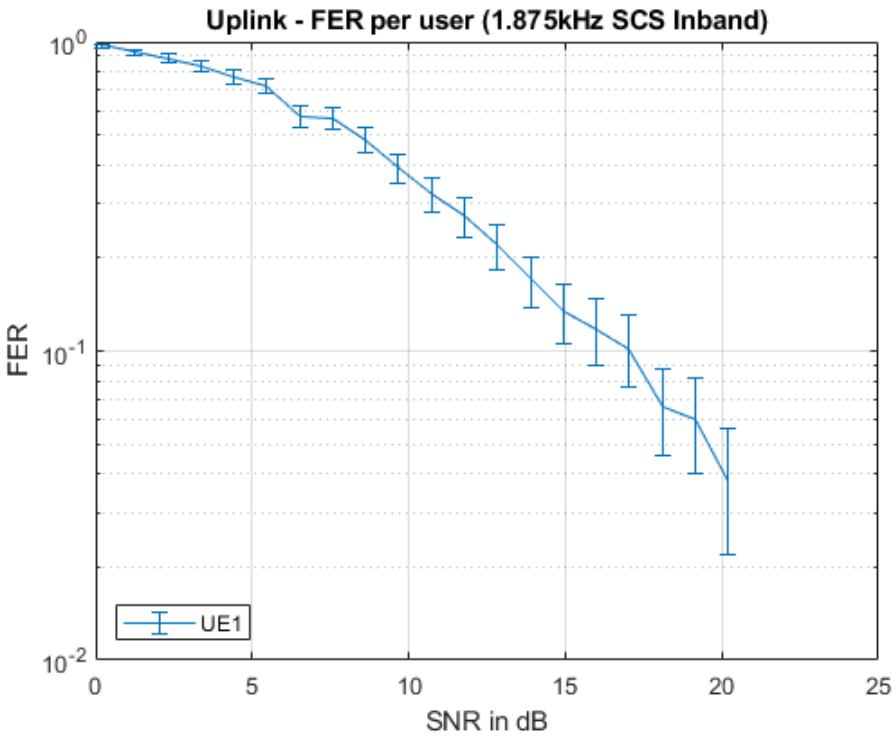

Fig 4.21: Our Proposed 1.875kHz SCS uplink BER in in-band mode

Result:

SCS \ SNR	0	5	10
15kHz	.9	.73	.35
3.75kHz	.9	.75	.37
1.875kHz	.95	.76	.38

Table 4.9: In-band FER comparison

4.2.3 In-band Throughput vs SNR:

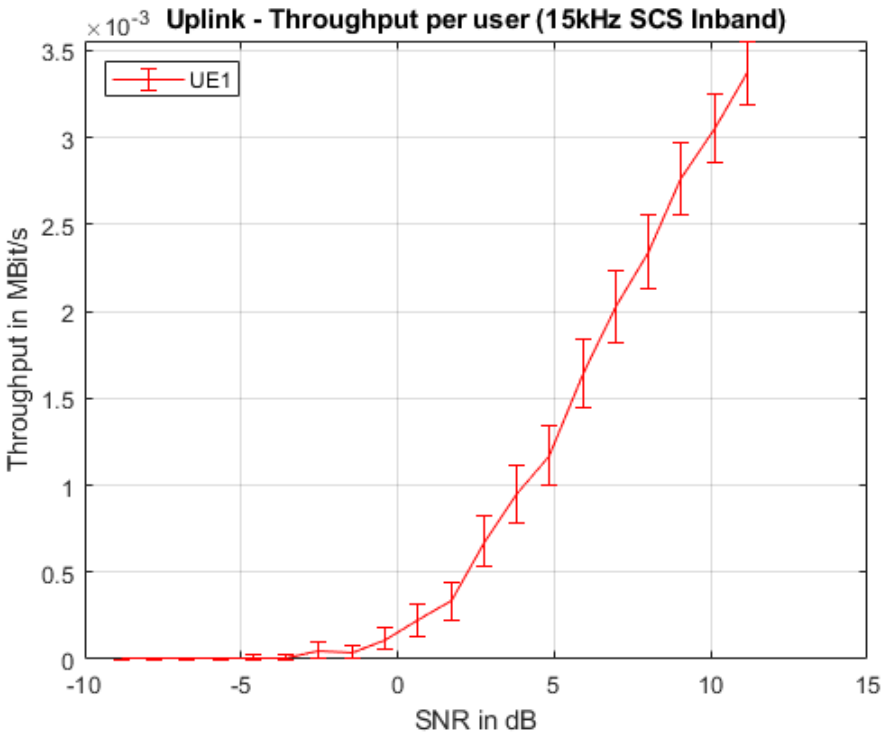

Fig 4.22: Already existing 15kHz SCS uplink throughput in in-band mode

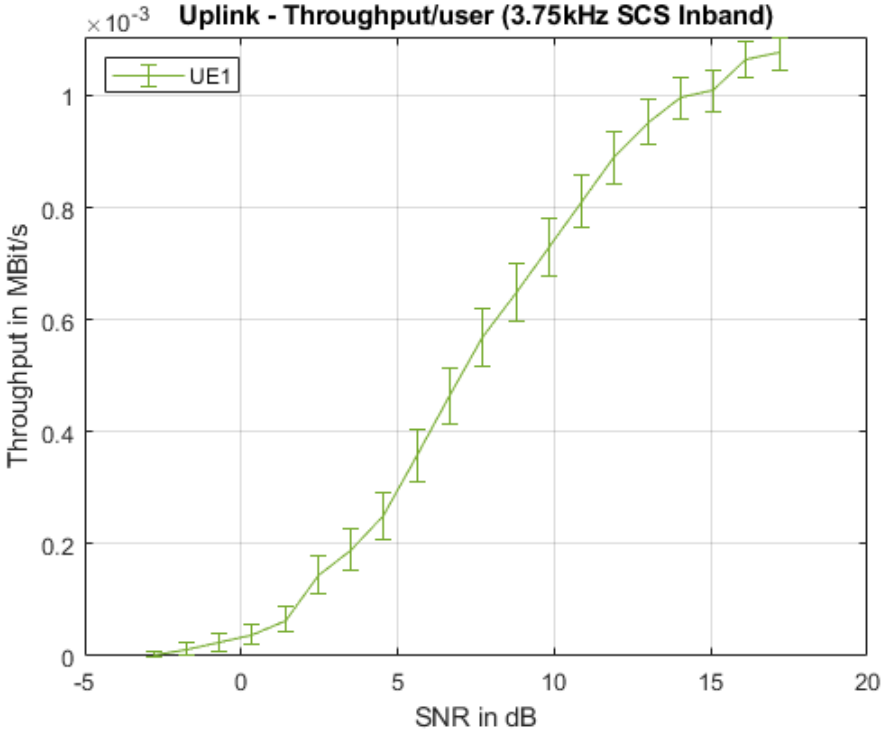

Fig 4.23: Already existing 3.75kHz SCS uplink throughput in in-band mode

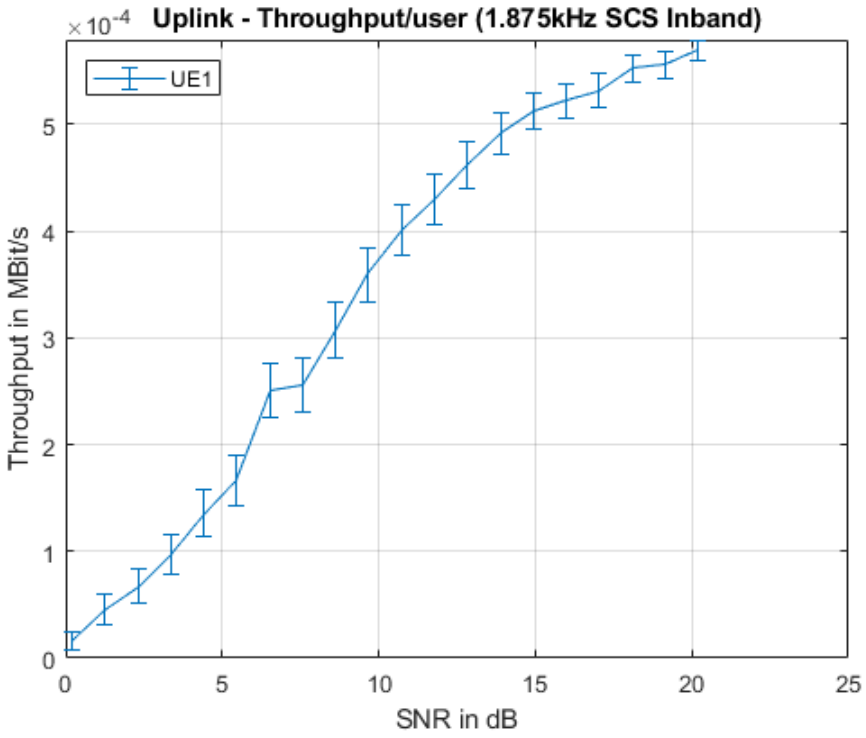

Fig 4.24: Our Proposed 1.875kHz SCS uplink throughput in in-band mode

Result:

SCS \ SNR	0	5	10
15kHz	.2e-3	1.2e-3	3e-3
3.75kHz	.12e-3	.3e-3	.73e-3
1.875kHz	.2e-4	1.5e-4	3.7e-4

Table 4.10: In-band throughput comparison

4.2.4 In-band CEE vs SNR:

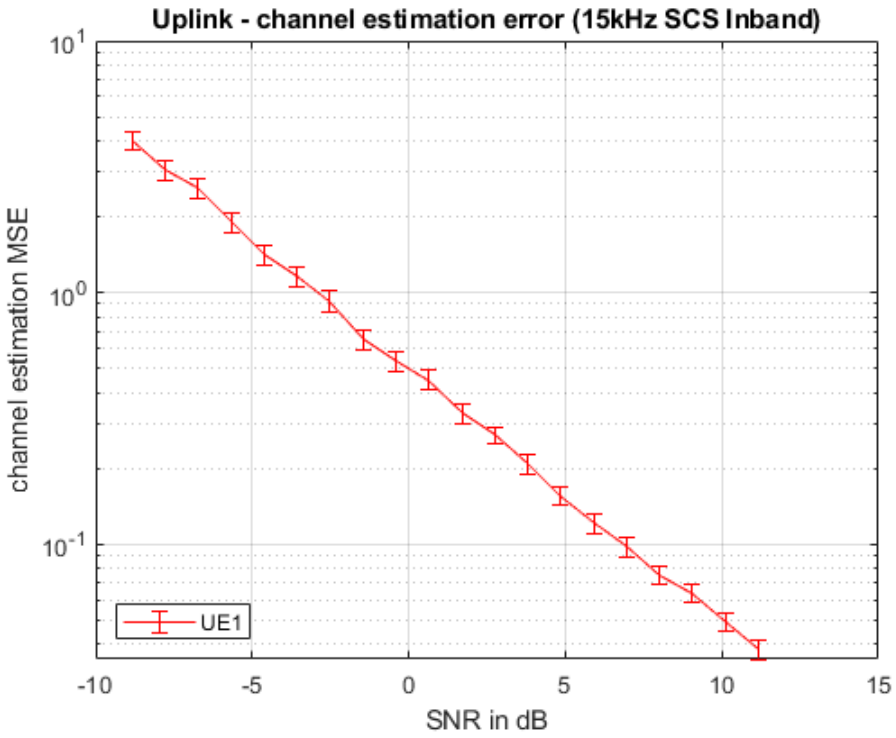

Fig 4.25: Already existing 15kHz SCS uplink CEE in in-band mode

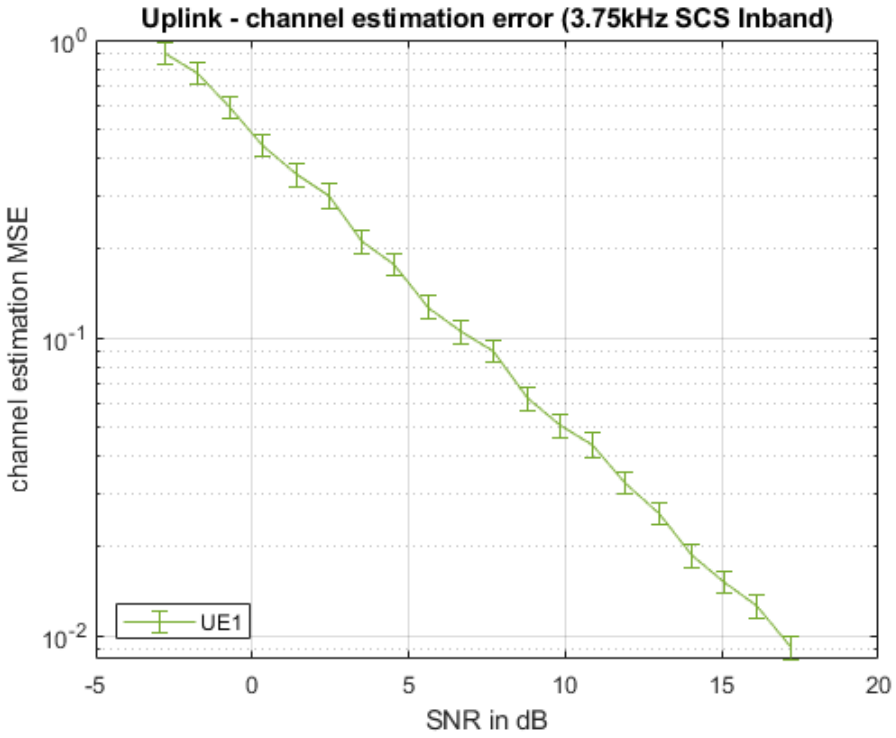

Fig 4.26: Already existing 3.75kHz SCS uplink CEE in in-band mode

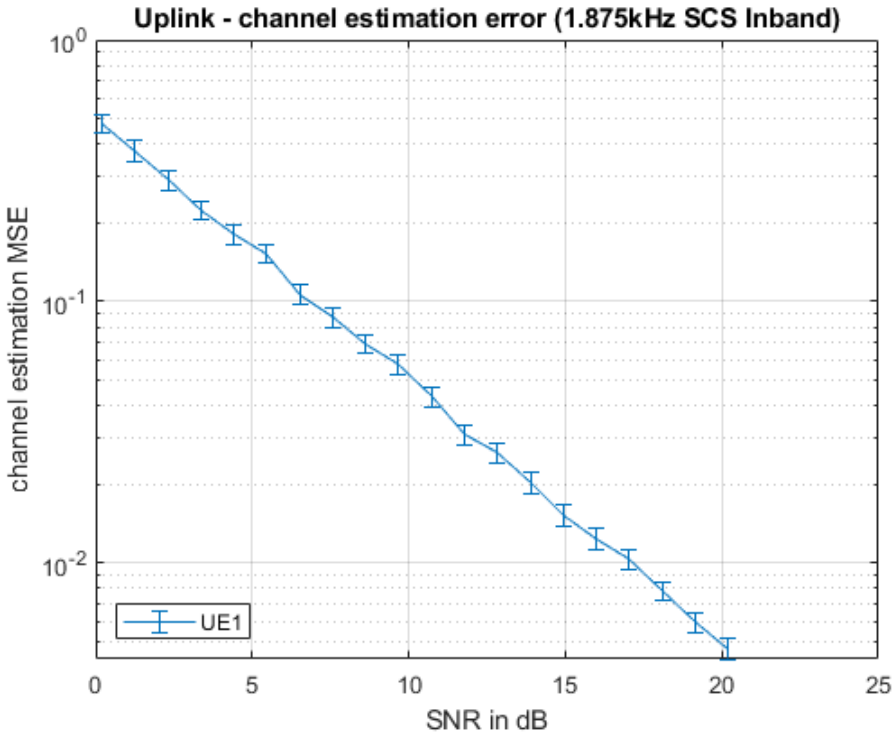

Fig 4.27: Our Proposed 1.875kHz SCS uplink CEE in in-band mode

Result:

SCS \ SNR	0	5	10
15kHz	.5	.16	.05
3.75kHz	.5	.17	.05
1.875kHz	.5	.17	.055

Table 4.11: In-band CEE comparison

4.2.5 In-band P vs PAPR:

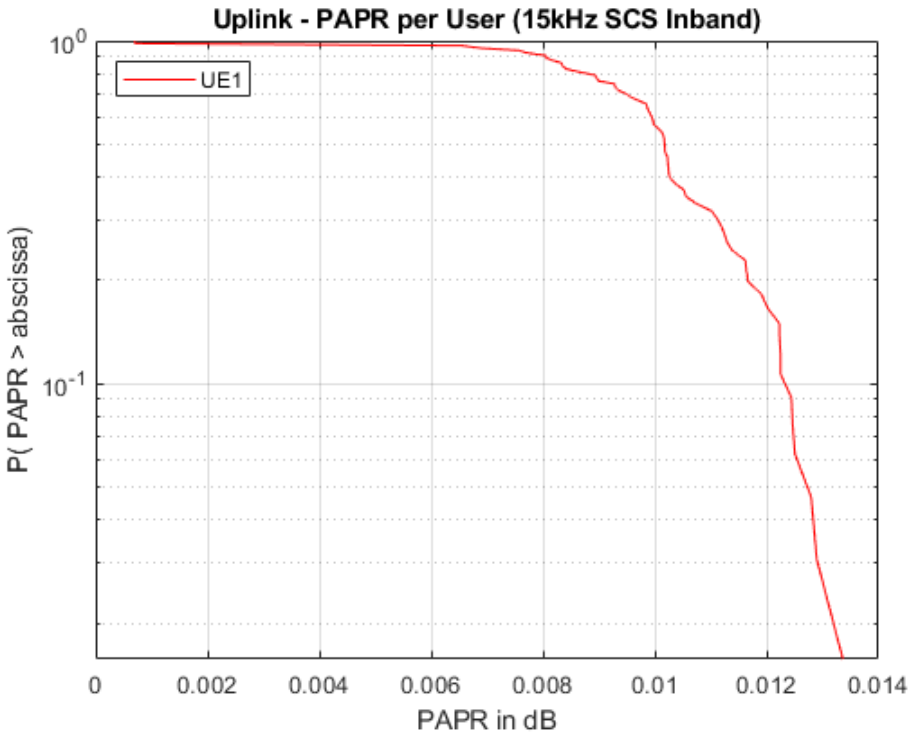

Fig 4.28: Already existing 15kHz SCS uplink PAPR in in-band mode

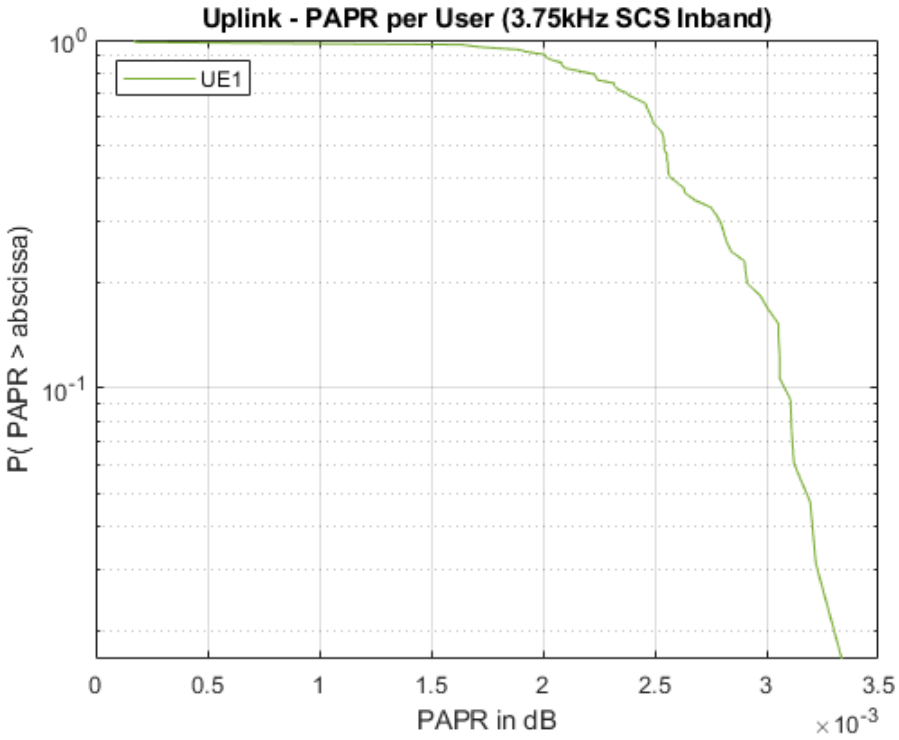

Fig 4.29: Already existing 3.75kHz SCS uplink PAPR in in-band mode

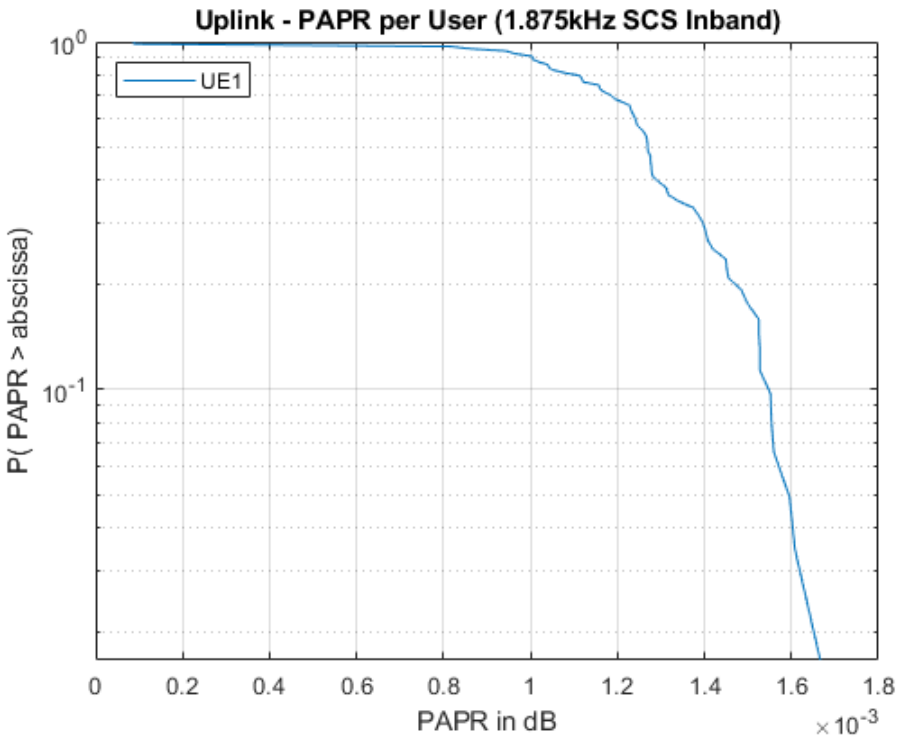

Fig 4.30: Our Proposed 1.875kHz SCS uplink PAPR in in-band mode

Result:

When PAPR is 1, PAPR in dB is 0. As PAPR is increasing, the probability CCDF function is decreasing. Thus, the probability of achieving the peak is decreasing.

P = 0.1 / SCS	At PAPR dB
15kHz	12.5e-3
3.75kHz	3.2e-3
1.875kHz	1.55e-3

Table 4.12: In-band PAPR comparison

4.3 Guard-band Deployment

Guard-band mode is used when the base station schedules NB-IoT PRBs in the guard bands between the LTE carriers. This mode is useful to avoid possible interference with LTE.

The Guard-band mode utilizes the LTE bands that are same as the in-band LTE bands. They are present in the TABLE 4.7.

For simulation, we have used the LTE-B85 band.
Simulation Guard-band Center Frequency: 707MHz.

4.3.1 Guard-band BER vs SNR:

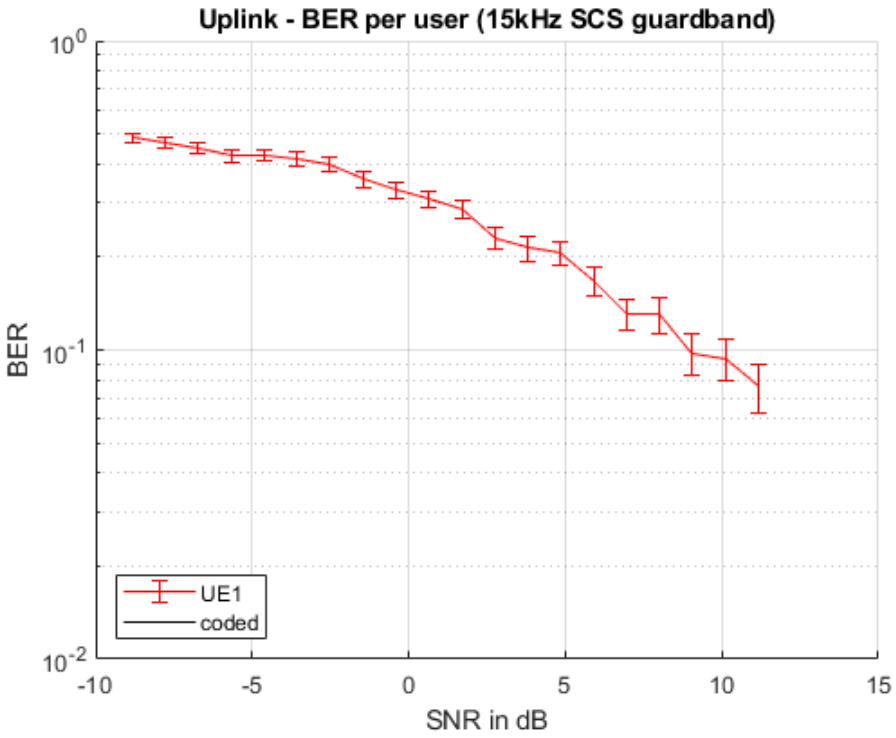

Fig 4.31: Already existing 15kHz SCS uplink BER in Guard-band mode

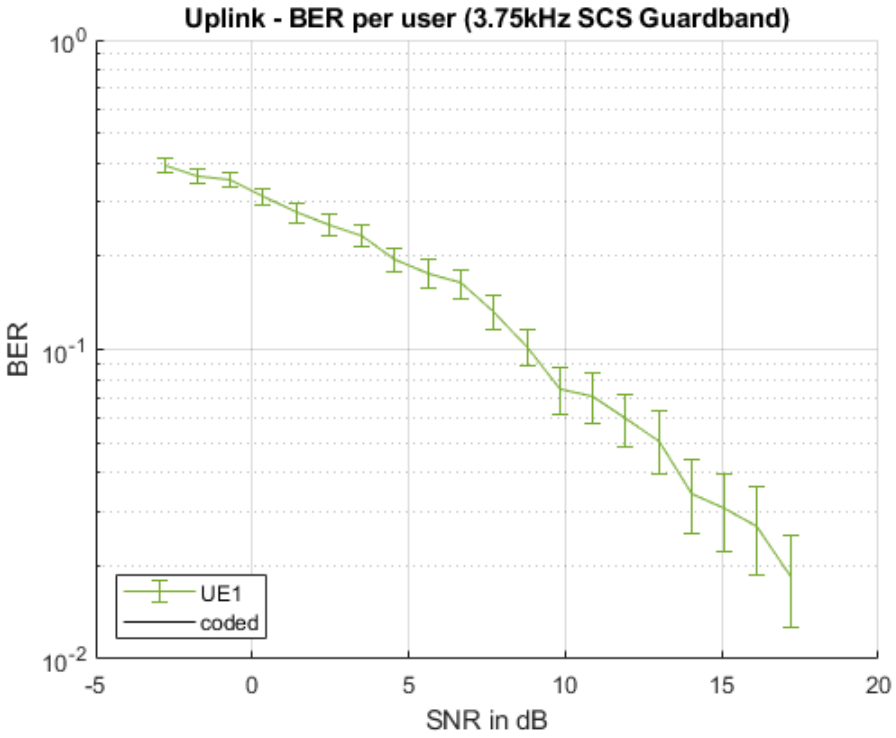

Fig 4.32: Already existing 3.75kHz SCS uplink BER in Guard-band mode

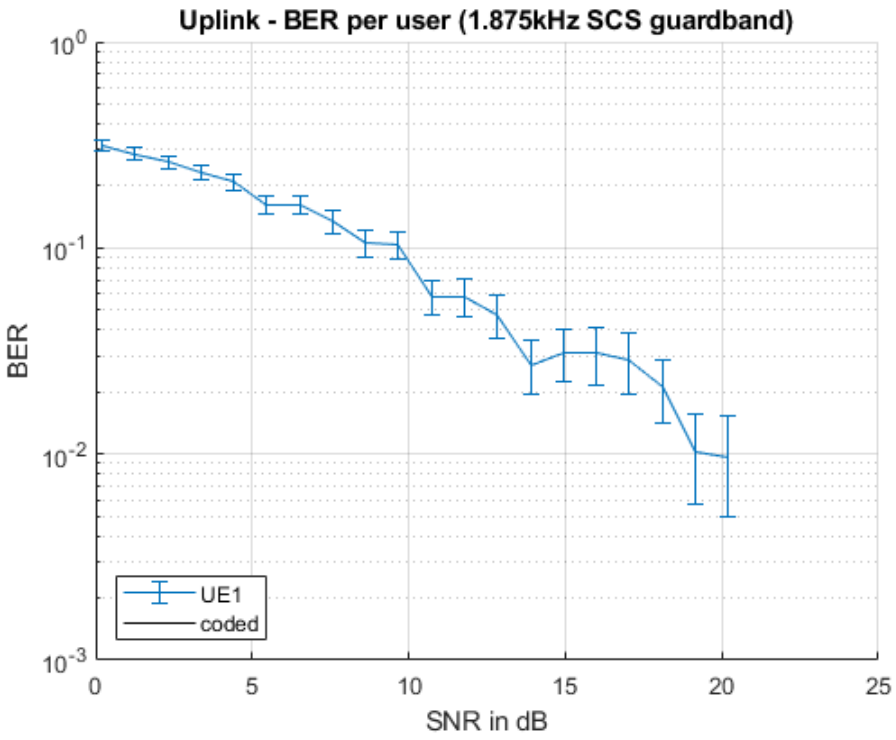

Fig 4.33: Our Proposed 1.875kHz SCS uplink BER in Guard-band mode

Result:

SCS \ SNR	0	5	10
15kHz	.32	.2	.092
3.75kHz	.34	.18	.075
1.875kHz	.3	.18	.031

Table 4.13: Guard-band BER comparison

4.3.2 Guard-band FER vs SNR:

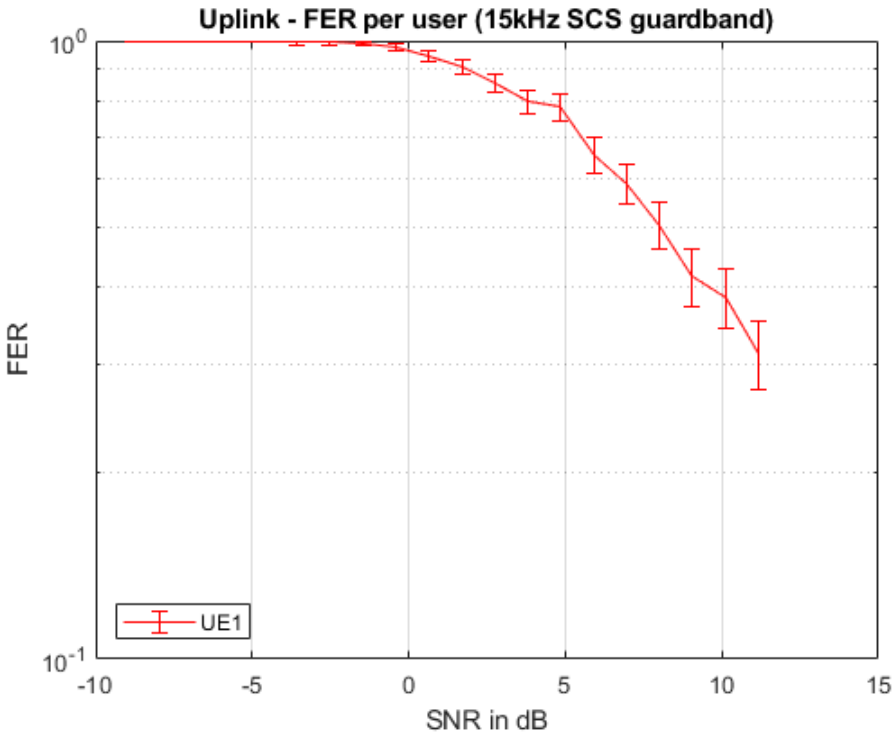

Fig 4.34: Already existing 15kHz SCS uplink FER in Guard-band mode

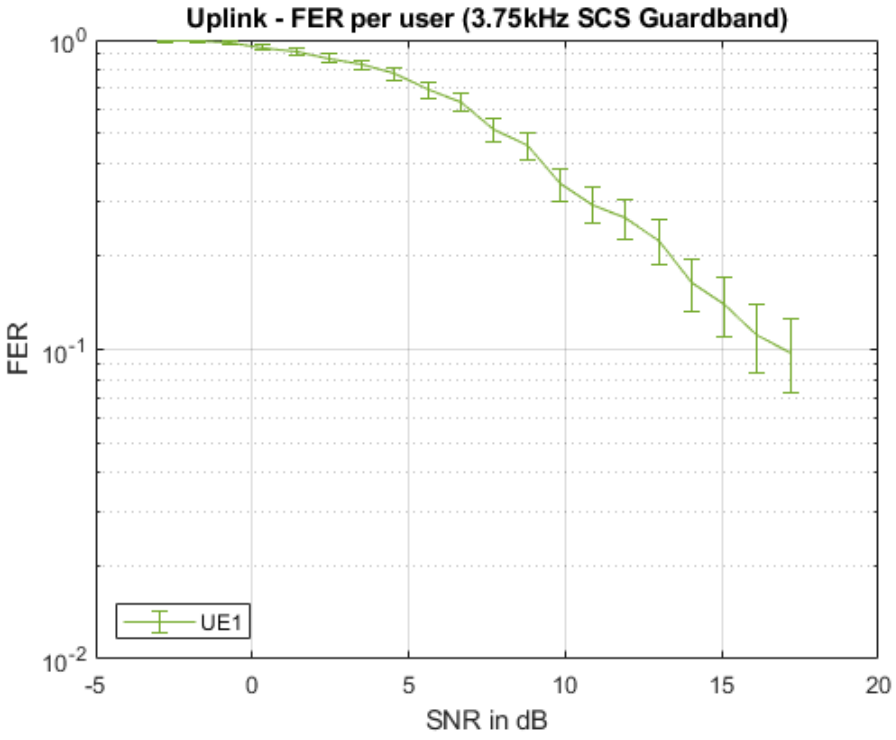

Fig 4.35: Already existing 3.75kHz SCS uplink FER in Guard-band mode

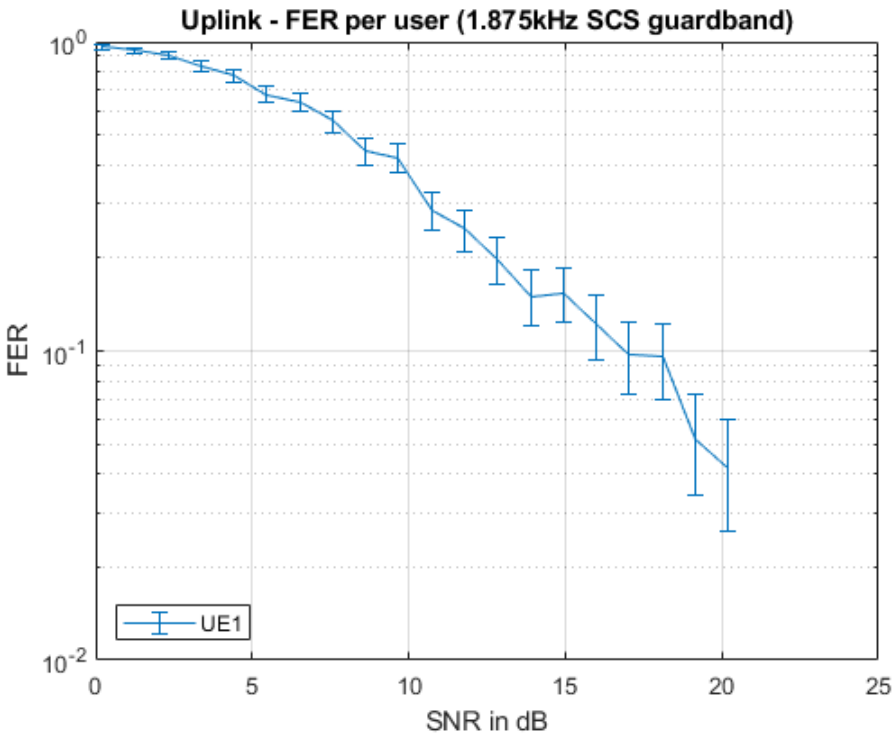

Fig 4.36: Our Proposed 1.875kHz SCS uplink FER in Guard-band mode

Result:

SCS \ SNR	0	5	10
15kHz	.9	.78	.38
3.75kHz	.9	.75	.35
1.875kHz	.9	.7	.39

Table 4.14: Guard-band FER comparison

4.3.3 Guard-band Throughput vs SNR:

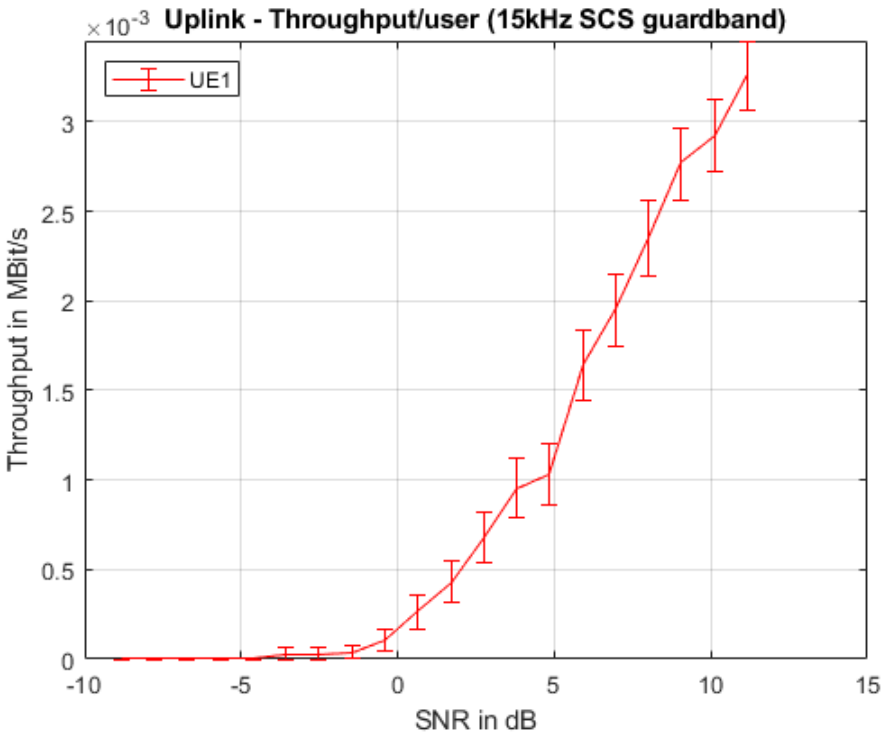

Fig 4.37: Already existing 15kHz SCS uplink throughput in Guard-band mode

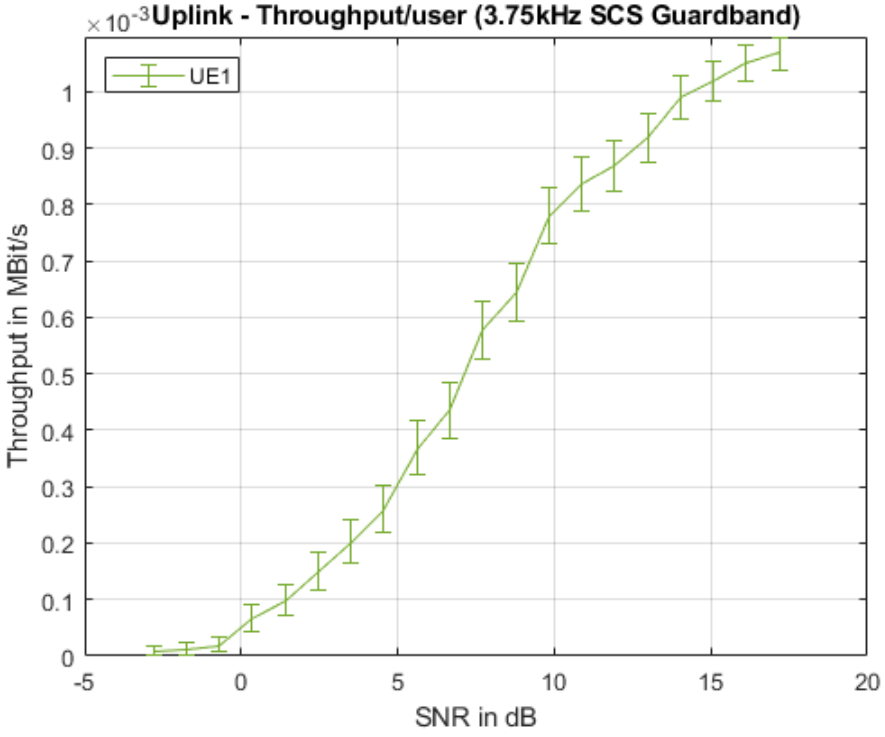

Fig 4.38: Already existing 3.75kHz SCS uplink throughput in Guard-band mode

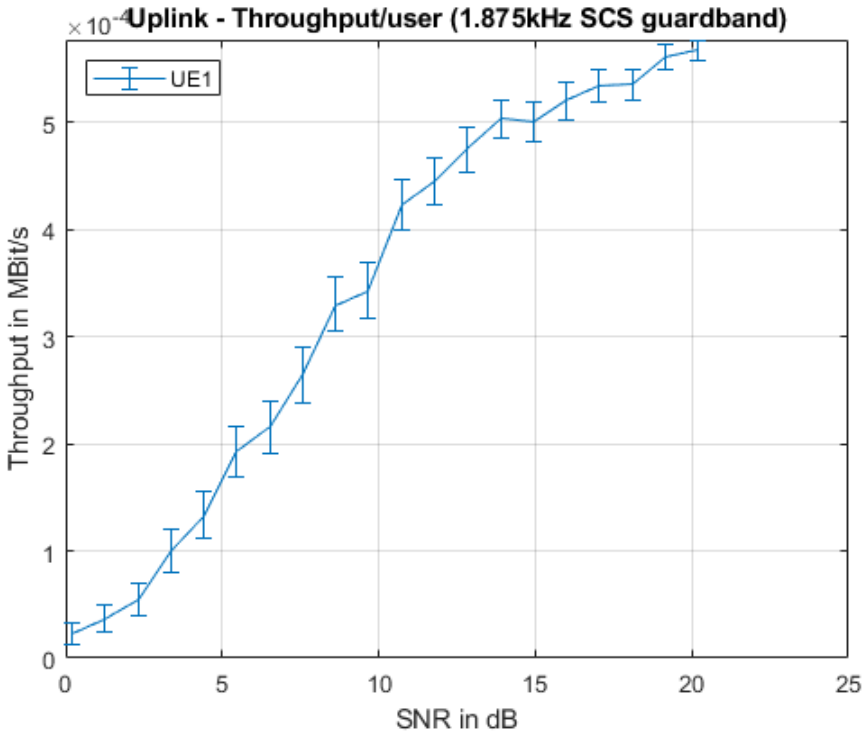

Fig 4.39: Our Proposed 1.875kHz SCS uplink throughput in Guard-band mode

Result:

SCS \ SNR	0	5	10
15kHz	.2e-3	1.1e-3	2.8e-3
3.75kHz	.05e-3	.3e-3	.78e-3
1.875kHz	.2e-4	1.5e-4	3.6e-4

Table 4.15: Guard-band throughput comparison

4.3.4 Guard-band CEE vs SNR:

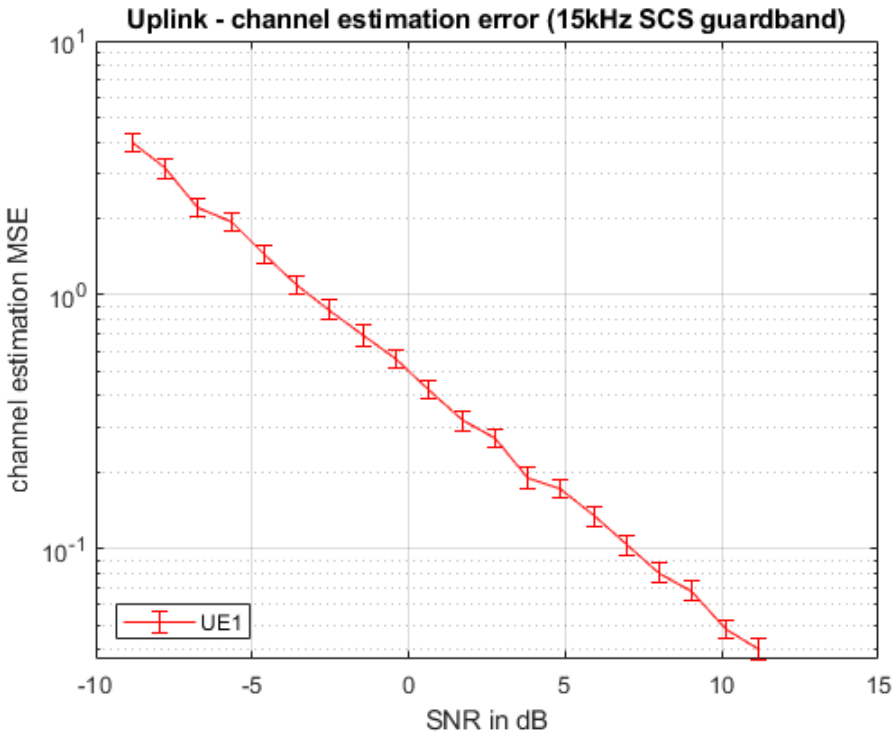

Fig 4.40: Already existing 15kHz SCS uplink CEE in Guard-band mode

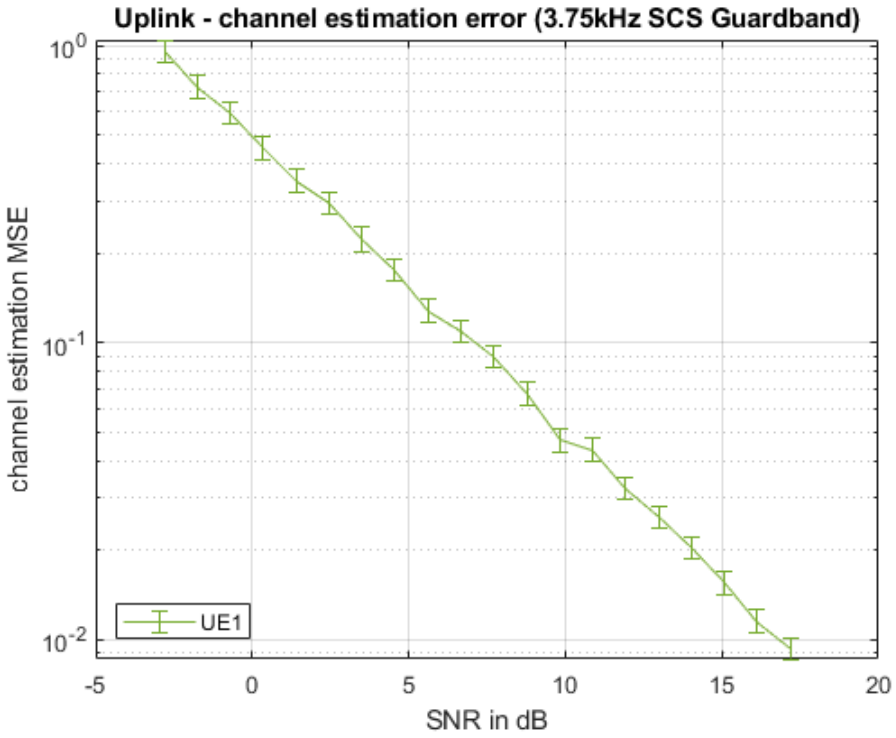

Fig 4.41: Already existing 3.75kHz SCS uplink CEE in Guard-band mode

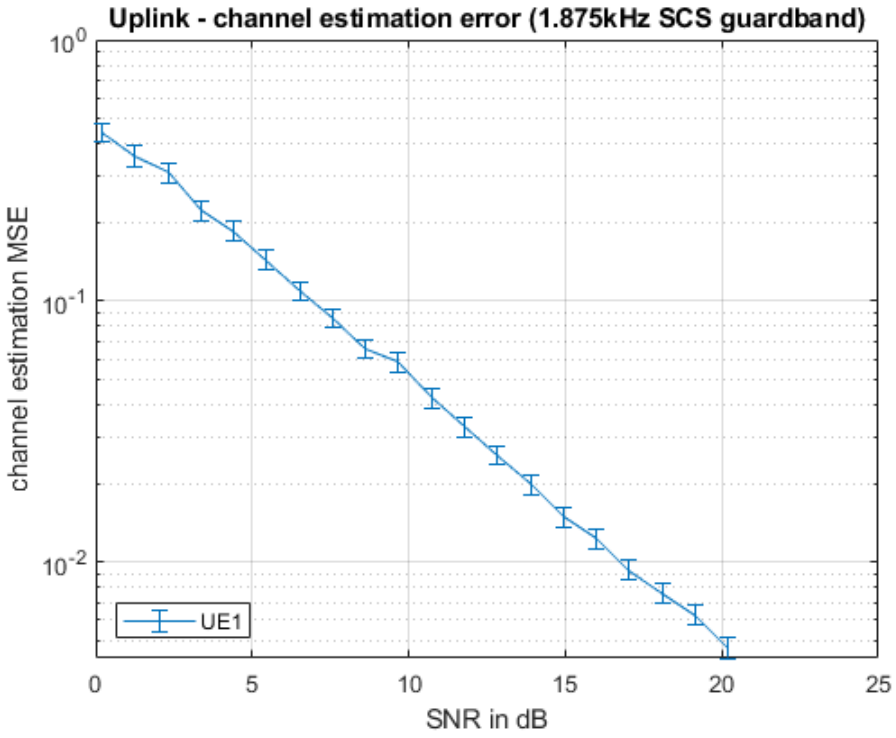

Fig 4.42: Our Proposed 1.875kHz SCS uplink CEE in Guard-band mode

Result:

SCS \ SNR	0	5	10
15kHz	.5	.18	.05
3.75kHz	.4	.16	.045
1.875kHz	.45	.17	.055

Table 4.16: Guard-band CEE comparison

4.3.5 Guard-band P vs PAPR:

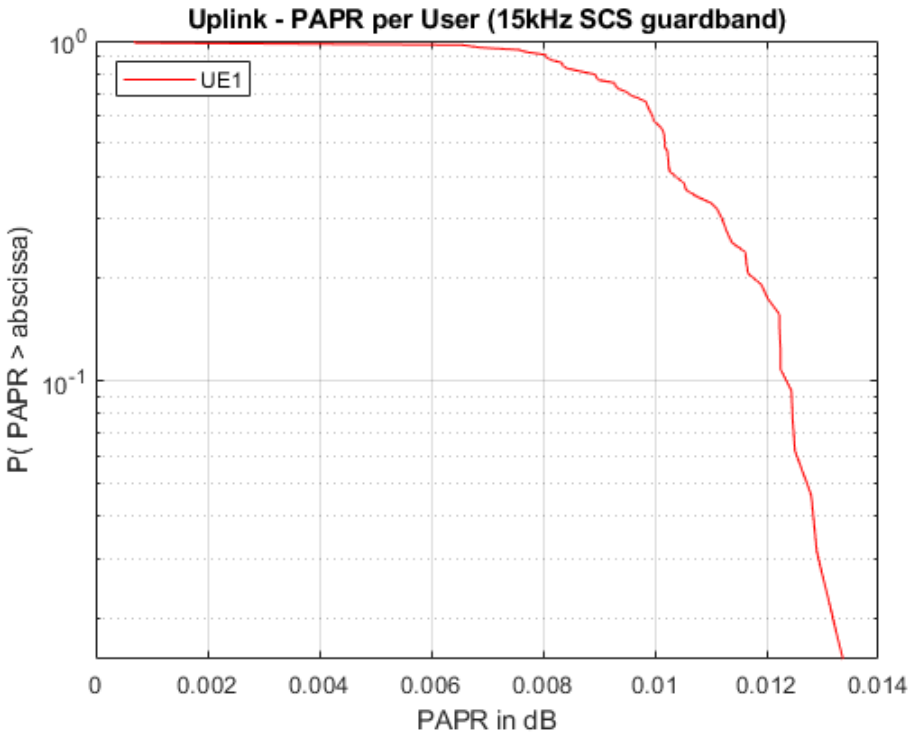

Fig 4.43: Already existing 15kHz SCS uplink PAPR in Guard-band mode

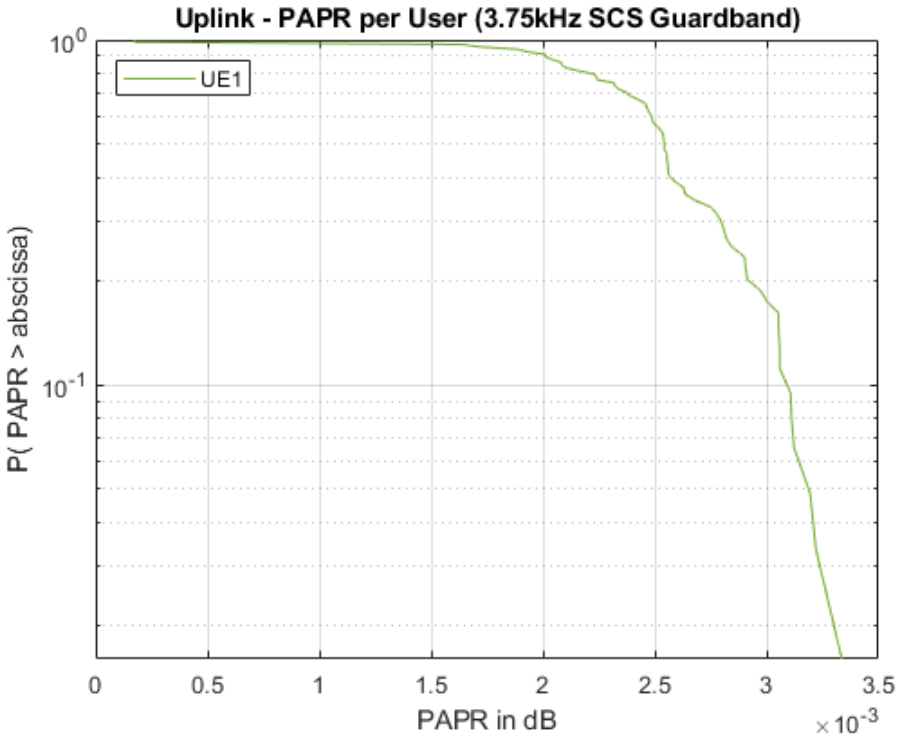

Fig 4.44: Already existing 3.75kHz SCS uplink PAPR in Guard-band mode

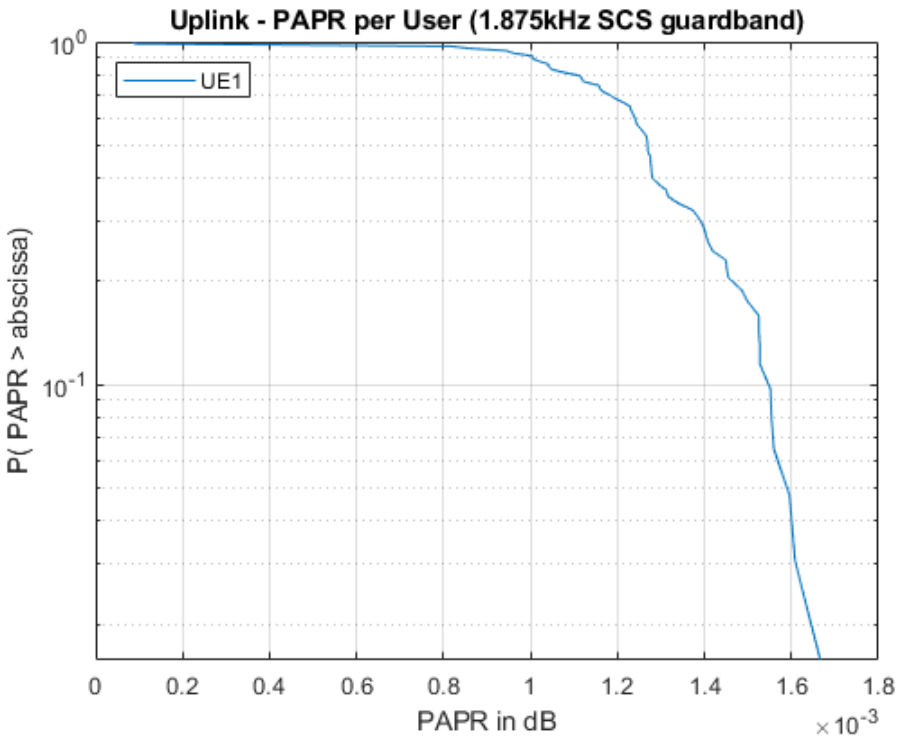

Fig 4.45: Our Proposed 1.875kHz SCS uplink PAPR in Guard-band mode

Result:

When PAPR is 1, PAPR in dB is 0. As PAPR is increasing, the probability CCDF function is decreasing. Thus, the probability of achieving the peak is decreasing.

P = 0.1 / SCS	At PAPR dB
15kHz	12.4e-3
3.75kHz	3.23e-3
1.875kHz	1.5e-3

Table 4.17: Guard-band PAPR comparison

Chapter 5

Conclusion

In order to materialize the revolutionary new world brought about by the Internet of Things, narrow band wireless links are as essential and efficient as ever. And OFDM seems to be the most solid and dependable option to achieve this interconnection. And as the number of device will be on the rise, the system must be able to accommodate this huge number of user devices. In this regard, our proposal is to reduce the subcarrier spacing to accommodate more device and increase the system capacity. So, we have proposed the 1.875kHz SCS and we have compared its link level performance to the already existing systems with 15kHz SCS and 1.875kHz SCS. Link level parameters such as BER, FER, throughput, CE error and PAPR have been simulated. Compared to the existing SCS systems, our proposed SCS system showed similar BER, FER and channel estimation error. For all the cases, the BER, FER and channel estimation error decrease as the SNR increases. The throughput also increases as the SNR increases. However, the throughput deteriorates when we reduce subcarrier spacing. In case of the PAPR curve, the probability reduces faster as we decrease the SCS. The probability for our proposed system drops the fastest.

For our future work, we would like to further reduce the subcarrier spacing to 0.9375kHz to increase the system capacity more. This will further increase the number of device accommodation in the OFDM system. OFDM has one of the most robust settings in the wireless connection technologies. So, we'd like to stick to it and engineer more efficient ways to increase the system capacity.

References

[1] A.-A. A. Boulogeorgos, P. D. Diamantoulakis, and G. K. Karagiannidis, “Low Power Wide Area Networks (LPWANs) for Internet of Things (IoT) Applications: Research Challenges and Future Trends,” no. November, 2016, [Online]. Available: http://arxiv.org/abs/1611.07449.

[2] Ericcson, “Ericsson Mobility Report - November 2020,” *Ericsson*, no. November, p. 36, 2020, [Online]. Available: https://www.ericsson.com/4adc87/assets/local/mobility-report/documents/2020/november-2020-ericsson-mobility-report.pdf.

[3] SigFox, “M2M and IoT redefined through cost effective and energy optimized connectivity,” *Whitepaper*, pp. 1–17, 2014.

[4] LoRa Alliance, “Mobile Experts White Paper for LoRa Alliance,” p. 9, 2015, [Online]. Available: https://www.lora-alliance.org/What-Is-LoRa/LoRaWAN-White-Papers.

[5] S. Dawaliby, A. Bradai, and Y. Pousset, “In depth performance evaluation of LTE-M for M2M communications,” pp. 1–8, 2017, doi: 10.1109/wimob.2016.7763264.

[6] M. Xiao *et al.*, “Millimeter Wave Communications for Future Mobile Networks,” *IEEE J. Sel. Areas Commun.*, vol. 35, no. 9, pp. 1909–1935, 2017, doi: 10.1109/JSAC.2017.2719924.

[7] Huawei, “NB-IOT White Paper - Enabling New Business Opportunities,” *Manual*, p. 23, 2017, [Online]. Available: https://www.huawei.com/minisite/iot/img/nb_iot_whitepaper_en.pdf.

[8] Z. DIng, X. Lei, G. K. Karagiannidis, R. Schober, J. Yuan, and V. K. Bhargava, “A Survey on Non-Orthogonal Multiple Access for 5G Networks: Research Challenges and Future Trends,” *IEEE J. Sel. Areas Commun.*, vol. 35, no. 10, pp. 2181–2195, 2017, doi: 10.1109/JSAC.2017.2725519.

[9] A. E. Mostafa, Y. Zhou, and V. W. S. Wong, “Connection Density Maximization of Narrowband IoT Systems with NOMA,” *IEEE Trans. Wirel. Commun.*, vol. 18, no. 10, pp. 4708–4722, 2019, doi: 10.1109/TWC.2019.2927666.

[10] S. Mishra, L. Salaun, and C. S. Chen, “Maximizing Connection Density in NB-IoT Networks with NOMA,” *IEEE Veh. Technol. Conf.*, vol. 2020-May, 2020, doi: 10.1109/VTC2020-Spring48590.2020.9129542.

[11] T. Xu and I. Darwazeh, “Non-Orthogonal Narrowband Internet of Things: A Design for Saving Bandwidth and Doubling the Number of Connected Devices,” *IEEE*

Internet Things J., vol. 5, no. 3, pp. 2120–2129, 2018, doi: 10.1109/JIOT.2018.2825098.

[12] T. Xu and I. Darwazeh, "Non-Orthogonal Waveform Scheduling for Next Generation Narrowband IoT," *2018 IEEE Globecom Work. GC Wkshps 2018 - Proc.*, no. 978, pp. 1–6, 2019, doi: 10.1109/GLOCOMW.2018.8644200.

[13] M. R. D. Rodrigues and I. Darwazeh, "Fast OFDM: A proposal for doubling the data rate of OFDM schemes," *Proceeding Int. Conf. Telecommun.*, no. June, pp. 484–487, 2003.

[14] P. Moakes, "5G New Radio Architecture and Challenges," *RF Glob.*, no. Dl, 2017, [Online]. Available: https://www.rfglobalnet.com/doc/g-new-radio-architecture-and-challenges-0001?vm_isPreview=true&user=cb8590bf-9377-4e03-8ea6-c6e315ef8984&utm_source=et_6214342&utm_medium=email&utm_campaign=RFG_11-30-2017&utm_term=cb8590bf-9377-4e03-8ea6-c6e315ef8984&utm_c.

[15] I. Darwazeh, H. Ghannam, and T. Xu, "The First 15 Years of SEFDM: A Brief Survey," *2018 11th Int. Symp. Commun. Syst. Networks Digit. Signal Process. CSNDSP 2018*, pp. 1–7, 2018, doi: 10.1109/CSNDSP.2018.8471886.

[16] T. Xu and I. Darwazeh, "Uplink Narrowband IoT Data Rate Improvement: Dense Modulation Formats or Non-Orthogonal Signal Waveforms?," *IEEE Int. Symp. Pers. Indoor Mob. Radio Commun. PIMRC*, vol. 2018-Septe, pp. 142–146, 2018, doi: 10.1109/PIMRC.2018.8580767.

[17] T. Xu and I. Darwazeh, "Spectrally efficient FDM: Spectrum saving technique for 5G?," *Proc. 2014 1st Int. Conf. 5G Ubiquitous Connect. 5GU 2014*, pp. 273–278, 2014, doi: 10.4108/icst.5gu.2014.258120.

[18] Z. Yin, M. Jia, F. Lyu, W. Wang, Q. Guo, and X. S. Shen, "Spectral efficiency analysis of SEFDM systems with ICI mitigation," *IEEE Veh. Technol. Conf.*, vol. 2019-Septe, pp. 1–5, 2019, doi: 10.1109/VTCFall.2019.8891303.

[19] Y. Ma, N. Wu, W. Yuan, D. W. K. Ng, and L. Hanzo, "Joint Channel Estimation and Equalization for Index-Modulated Spectrally Efficient Frequency Division Multiplexing Systems," *IEEE Trans. Commun.*, vol. 68, no. 10, pp. 6230–6244, 2020, doi: 10.1109/TCOMM.2020.3007387.

[20] H. Ghannam and I. Darwazeh, "Robust channel estimation methods for spectrally efficient FDM systems," *IEEE Veh. Technol. Conf.*, vol. 2018-June, pp. 1–6, 2018, doi: 10.1109/VTCSpring.2018.8417823.

[21] "3GPP TR 36.802 V13.0.0,"Evolved Universal Terrestrial Radio Access (E-UTRA);

NB-IOT; Technical Report for BS and UE radio transmission and reception (Release 13)"." .

[22] E. Rastogi, N. Saxena, A. Roy, and D. R. Shin, "Narrowband Internet of Things: A Comprehensive Study," *Comput. Networks*, vol. 173, no. February, p. 107209, 2020, doi: 10.1016/j.comnet.2020.107209.

[23] H. Fattah, *5G LTE Narrowband Internet of Things (NB-IoT)*, 1st ed. USA: CRC Press, Inc., 2018.

[24] 3GPP, "TS 136 101 - V8.2.0 - LTE; Evolved Universal Terrestrial Radio Access (E-UTRA); User Equipment (UE) radio transmission and reception (3GPP TS 36.101 version 8.2.0 Release 8)," *Eur. Telecommun.*, vol. 0, 2016.

[25] T. Specification, "TS 136 307 - V9.2.0 - LTE; Evolved Universal Terrestrial Radio Access (E-UTRA); Requirements on User Equipments (UEs) supporting a release-independent frequency band (3GPP TS 36.307 version 9.2.0 Release 9)," vol. 0, pp. 0–11, 2011.

[26] L. Feltrin *et al.*, "Narrowband IoT: A survey on downlink and uplink perspectives," *IEEE Wirel. Commun.*, vol. 26, no. 1, pp. 78–86, 2019, doi: 10.1109/MWC.2019.1800020.

[27] R. Ratasuk, N. Mangalvedhe, J. Kaikkonen, and M. Robert, "Data channel design and performance for LTE narrowband IoT," *IEEE Veh. Technol. Conf.*, vol. 0, pp. 0–4, 2016, doi: 10.1109/VTCFall.2016.7880951.

[28] J. Xu, J. Yao, L. Wang, Z. Ming, K. Wu, and L. Chen, "Narrowband Internet of Things : Evolutions , Technologies and Open Issues," vol. 4662, no. c, pp. 1–13, 2017, doi: 10.1109/JIOT.2017.2783374.

[29] M. S. Ali, Y. Li, M. K. H. Jewel, O. J. Famoriji, and F. Lin, "Channel Estimation and Peak-to-Average Power Ratio Analysis of Narrowband Internet of Things Uplink Systems," *Wirel. Commun. Mob. Comput.*, vol. 2018, 2018, doi: 10.1155/2018/2570165.

[30] C. Yu, L. Yu, Y. Wu, Y. He, and Q. Lu, "Uplink scheduling and link adaptation for narrowband internet of things systems," *IEEE Access*, vol. 5, pp. 1724–1734, 2017, doi: 10.1109/ACCESS.2017.2664418.

[31] T. Specification, "TS 136 211 - V14.9.0 - LTE; Evolved Universal Terrestrial Radio Access (E-UTRA); Physical channels and modulation (3GPP TS 36.211 version 14.9.0 Release 14)," vol. 0, pp. 0–121, 2014, [Online]. Available: https://portal.etsi.org/TB/ETSIDeliverableStatus.aspx.

[32] E. U. Terrestrial, “TS 136 300 - V13.12.0 - LTE; Evolved Universal Terrestrial Radio Access (E-UTRA) and Evolved Universal Terrestrial Radio Access Network (E-UTRAN); Overall description; Stage 2 (3GPP TS 36.300 version 13.12.0 Release 13),” vol. 0, 2018.

[33] T. Specification, “TS 136 211 - V11.5.0 - LTE; Evolved Universal Terrestrial Radio Access (E-UTRA); Physical channels and modulation (3GPP TS 36.211 version 11.5.0 Release 11),” vol. 0, pp. 0–121, 2014, [Online]. Available: https://portal.etsi.org/TB/ETSIDeliverableStatus.aspx.

[34] M. Kanj, V. Savaux, and M. Le Guen, “A Tutorial on NB-IoT Physical Layer Design,” *IEEE Commun. Surv. Tutorials*, vol. 22, no. 4, pp. 2408–2446, 2020, doi: 10.1109/COMST.2020.3022751.

[35] Y. P. E. Wang *et al.*, “A Primer on 3GPP Narrowband Internet of Things,” *IEEE Commun. Mag.*, vol. 55, no. 3, pp. 117–123, 2017, doi: 10.1109/MCOM.2017.1600510CM.

[36] H. Malik, H. Pervaiz, M. Mahtab Alam, Y. Le Moullec, A. Kuusik, and M. Ali Imran, “Radio Resource Management Scheme in NB-IoT Systems,” *IEEE Access*, vol. 6, pp. 15051–15064, 2018, doi: 10.1109/ACCESS.2018.2812299.

[37] T. Specification, “TS 136 211 V15.5.0 - LTE; Evolved Universal Terrestrial Radio Access (E-UTRA); Physical layer procedures (3GPP TS 36.213 version 13.4.0 Release 13),” *Eur. Telecommun.*, vol. 0, pp. 0–78, 2009, [Online]. Available: https://portal.etsi.org/TB/ETSIDeliverableStatus.aspx.

[38] “Energy Efficiency for NPUSCH in NB-IoT with Guard Band,” vol. 16, no. 4, pp. 1–6, 2018, doi: 10.19729/j.cnki.1673.

[39] “R1-160145 Discussion of Uplink DMRS Design.” [Online]. Available: https://www.3gpp.org/ftp/tsg_ran/WG1_RL1/TSGR1_AH/LTE_NB-IoT_1601/Docs.

[40] https://www.ubiik.com/lpwan-technology

[41] https://halberdbastion.com/technology/iot/iot-protocols/ec-gsm-iot